BROADBAND PLASMA WAVES IN THE MAGNETOPAUSE AND POLAR CAP BOUNDARY LAYERS

G.S. LAKHINA[1,⋆] and B.T. TSURUTANI[2]
[1]*Indian Institute of Geomagnetism, Colaba, Mumbai - 400 005, India*
(E-mail: lakhina@iig.iigm.res.in);
[2]*Jet Propulsion Laboratory, Pasadena, California, USA*
(E-mail: btsurutani@jplsp.jpl.nasa.gov)

Abstract. Boundary layers occurring in the magnetosphere can support a wide spectrum of plasma waves spanning a frequency range of a few mHz to tens of kHz and beyond. This review describes the main characteristics of the broadband plasma waves observed in the Earth's low-latitude magnetopause boundary layer (LLBL), in the polar cap boundary layer (PCBL), and the possible generation mechanisms. The broadband waves at the low-latitude boundary layer are sufficiently intense to cause the diffusion of the magnetosheath plasma across the closed magnetospheric field lines at a rate rapid enough to populate and maintain the boundary layer itself. The rapid pitch angle scattering of energetic particles via cyclotron resonant interactions with the waves can provide sufficient precipitation energy flux to the ionosphere to create the dayside aurora. In general, the broadband plasma waves may play an important part in the processes of local heating/acceleration of the boundary layer plasma.

Keywords: plasma waves, boundary layer waves, broadband waves

1. Introduction

The geomagnetic field forms an obstacle in a super-Alfvénic and supersonic solar wind flow as the solar wind approaches the Earth. As a result a standing shock wave is formed which heats, compresses, and deflects the oncoming solar wind plasma smoothly around the Earth. The region of shocked solar wind plasma downstream of the bow-shock is known as the magnetosheath. The magnetopause is the boundary which separates shocked solar wind plasma in the magnetosheath from the hot plasma in the magnetosphere. Several plasma measurements have identified the existence of a boundary layer, inside of and adjacent to the magnetopause, consisting of plasma with temperature and flow properties intermediate between the magnetosheath and the magnetosphere proper (Hones et al., 1972; Akasofu et al., 1973; Eastman et al., 1976; Haerendel et al., 1978). This boundary layer is referred to as the magnetospheric boundary layer (Eastman et al., 1976; Lundin, 1987). The magnetospheric boundary layer extends over the entire known portion

⋆ *Address for correspondence:* G.S. Lakhina, Indian Institute of Geomagnetism, Dr. Nanabhai Moos Marg, Colaba, Mumbai – 400 005, India. Fax: +91 22 218 9568.

Surveys in Geophysics **20:** 377–414, 1999.

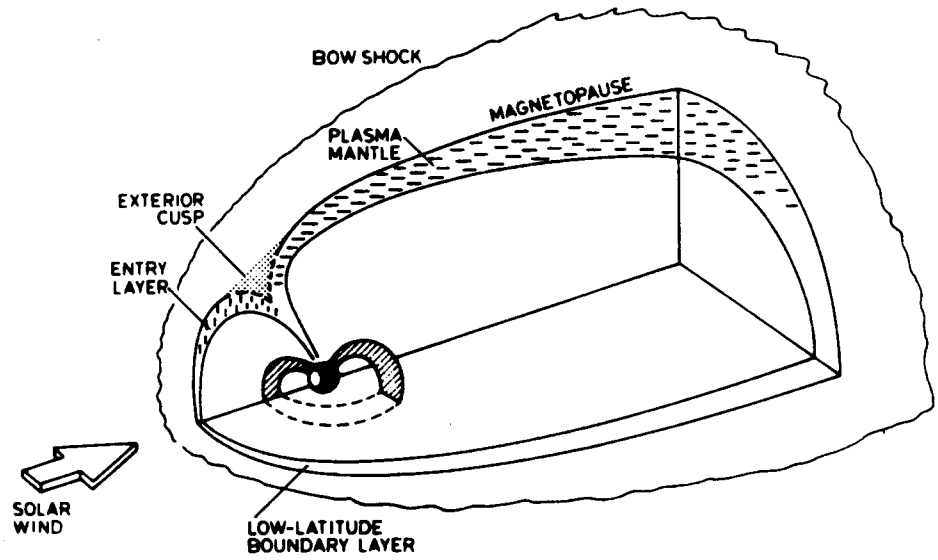

Figure 1. Schematics of the Earth's magnetosphere with its magnetospheric boundary layers. The plasma mantle, the exterior cusp, the entry layer, and the low-latitude boundary layer are indicated. From Lundin (1987, Figure 1]).

of the magnetopause, but its properties differ considerably from one region to another. At low latitudes, the boundary layer thickness is typically a few hundred to a few thousand kilometers. The low latitude portion of this boundary layer is known as the low latitude boundary layer (LLBL) and the high latitude part as the high latitude boundary layer (HLBL) which includes the plasma mantle (PM), entry layer (EL) and the polar cusp (PC) (Hones et al., 1972; Rosenbauer et al., 1975; Eastman et al. 1976; and Haerendel and Paschmann, 1982). Figure 1 shows various regions of the magnetospheric boundary layer.

The magnetopause boundary layer plays an important role in transferring solar wind energy and momentum into the magnetosphere. Solar wind plasma can cross the magnetopause and enter the magnetosphere either by a direct entry due to flow along reconnected, open field lines or by cross-field transport due to scattering across closed magnetopause field lines (Tsurutani and Thorne, 1982; Baumjohann and Paschmann, 1987). The first process is more likely to be important when the interplanetary magnetic field (IMF) is directed southward. In this case the solar wind and magnetospheric field lines are anti-parallel which is an ideal situation for the magnetic reconnection to occur. Magnetic reconnection, due to southward directed field leads to 5 to 10% solar wind ram energy input into the Earth's magnetosphere (Weiss et al., 1992; Gonzalez et al., 1989) during substorms and storms. However, the energy injection efficiency is considerably less during northward IMF intervals. Under these situations, the wave-particle cross-field transport can be important. It

is found that during northward IMF about 0.1 to 0.3% of the ram energy can be transferred to the magnetosphere (Tsurutani and Gonzalez, 1995).

The magnetopause boundary layer can support a wide spectrum of plasma waves spanning a frequency range of a few mHz to tens of kHz and beyond. These boundary layer waves can play an important role in the cross-field transport processes. These waves can diffuse the magnetosheath plasma across the closed magnetospheric field lines at a rate rapid enough to create the low latitude boundary layer (LLBL) itself (Tsurutani and Thorne, 1982; Gendrin, 1979, 1983; Thorne and Tsurutani, 1991). This would provide a specific mechanism for "viscous interaction" (Axford and Hines, 1961; Eviatar and Wolf, 1968; Tsurutani and Gonzalez, 1995) in which the solar wind flow energy is transferred to the magnetosphere. It has been shown that cyclotron resonant interactions of these waves with the energetic particles can put protons and electrons on near-strong to strong pitch angle diffusion to create the dayside aurora at the Earth (Tsurutani et al., 1981), a phenomenon that is ever present and is independent of substorms. Treumann et al. (1991) have also shown that broadband plasma waves have large enough power to explain the boundary layer formation during nonreconnecting times. Cattell et al. (1995) concluded that the amplitudes of the magnetopause boundary layer waves were large enough to provide the dissipation required for reconnection to occur.

Recent POLAR plasma wave observations indicated that similar waves are present on magnetic field lines that penetrate the LLBL but are near the POLAR apogee of 6–8R_E and also near the POLAR perigee at $\sim$ 2R_E (Pickett et al., 1997; Ho et al., 1997; Tsurutani et al., 1998). The region of wave activity bounds the dayside (05 and 18 MLT, where MLT is the magnetic local time) polar cap magnetic field lines; thus these waves are called polar cap boundary layer (PCBL) waves. Here we shall review the characteristics of high-frequency (wave frequency, $f > 1$ Hz) broadband plasma waves observed in the magnetopause boundary and in the polar cap boundary layers. In both the regions, the waves could play a crucial role in the heating, acceleration and cross-field diffusion of the electrons and ions. Section 2 describes the broadband plasma waves observed in the Earth's magnetopause boundary layer, and their possible role in the cross-field particle transport which sustains the boundary layer itself and in the formation of dayside aurora. Section 3 deals with the PCBL boundary layer waves. Various possible generation mechanisms for the boundary layer waves are discussed in Section 4. Section 5 summarizes the results, and gives a brief description of the latest results on the high time resolution of the broadband plasma waves.

2. Earth Magnetopause Boundary Layer

2.1. BROADBAND PLASMA WAVE OBSERVATIONS

The Earth's magnetopause is a complex variable boundary. The earlier studies on the wave phenomena at the magnetopause were concerned with the observations of ultra-low frequency (ULF) waves (Holzer et al., 1966; Anderson et al., 1968; Cummings and Coleman, 1968; Smith and Davis, 1970; Aubry et al., 1971). The long period oscillations are thought to be generated either by the magnetopause boundary motions or by the Kelvin–Helniholtz instabilities, tearing instabilities, or by drift wave type instabilities (Holzer et al., 1966; Miura, 1987; Sckopke et al., 1981; Lakhina et al., 1993; Anderson, 1995; Lakhina and Schindler, 1996). Whistler-mode waves were reported by Neugebauer et al. (1974) using wave magnetic field measurements from OGO-5. Magnetic waves near the ion cyclotron frequency ($f_{ci} \approx 1$ Hz) were reported by Fairfield (1976) from IMP 6 magnetic field measurements. From the HEOS-2 magnetic measurements, Bahsen (1978) showed that the wave amplitudes, in the frequency range 20–235 Hz, peaked at the magnetopause, and the power spectral density falls off with increasing frequency. Here we will focus mainly on the high frequency plasma waves ($f > 1$ Hz) observed at the magnetopause.

Gurnett et al. (1979) were the first to report the results on both the plasma wave electric and magnetic fields in the vicinity of the magnetopause using measurements from the ISEE 1 and 2 spacecrafts. They found that the maximum plasma wave intensities usually occur at the magnetopause. An example is shown in Figure 2. They observed magnetic waves in the frequency range of 5.6 Hz to 1 kHz characterized by an $f^{-3.3}$ power law spectrum. The electric field turbulence occurred in the frequency range 5.6 Hz to 100 kHz and had a featureless spectrum obeying an $f^{-2.2}$ power law. Figure 3 shows typical electric and magnetic field spectra of the magnetopause boundary layer waves. In a few cases, Gurnett et al. (1979) could determine the polarization of the wave electric field from the spin modulation of the electric field intensity. In cases where spin modulation was clearly present, the electric field had perpendicular polarization. Gurnett et al. (1979) suggested that the magnetic waves are whistler mode waves, and that the electric component is a superposition of some electrostatic emissions and the electric component of the whistler mode. Tsurutani et al. (1981) studied 10 ISEE 1 and 2 magnetopause crossings and found an average magnetic wave spectrum to be $10 f^{-3.9}$ nT^2 Hz^{-1} for the frequency range of (10–1000) Hz. A typical electric waves spectrum in the frequency range (10–10^5) Hz was characterized by $3 \times 10^{-5} f^{-2.8}$ V^2 m^{-2} Hz^{-1}. However, both the spectra varied by an order of magnitude in amplitude from case to case. Anderson et al. (1982) studied the morphology of plasma waves associated with the magnetopause, from the magnetosheath to the outer magnetosphere using high time resolution measurements from ISEE 1 and 2. They found little difference

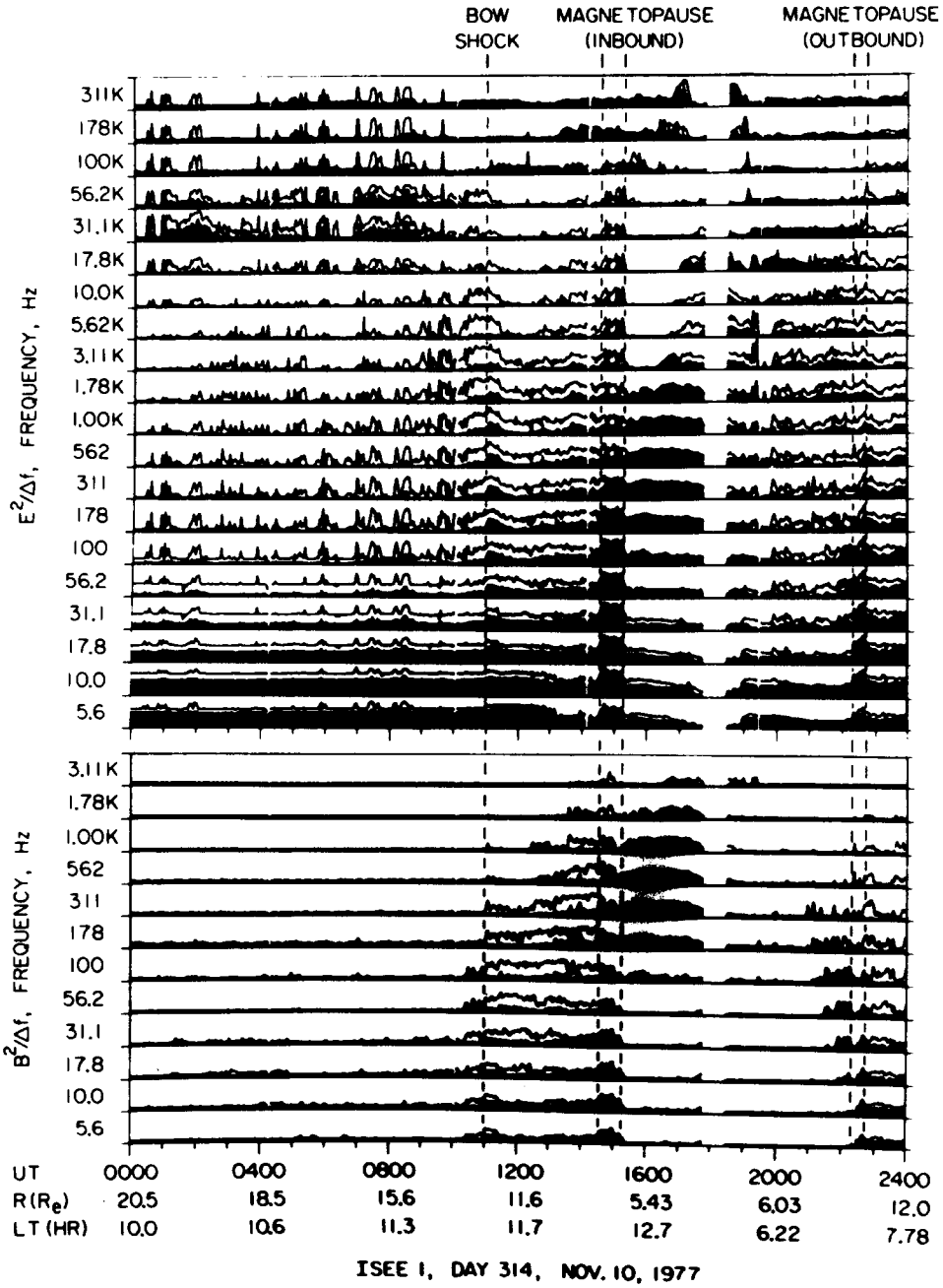

Figure 2. The plasma wave electric and magnetic field data from ISEE 1 for a representative pass through the magnetospere. The enhanced electric and magnetic field intensities at the inbound and outbound magnetopause crossings are clearly indicated. From Gurnett et al. (1979, Figure 1).

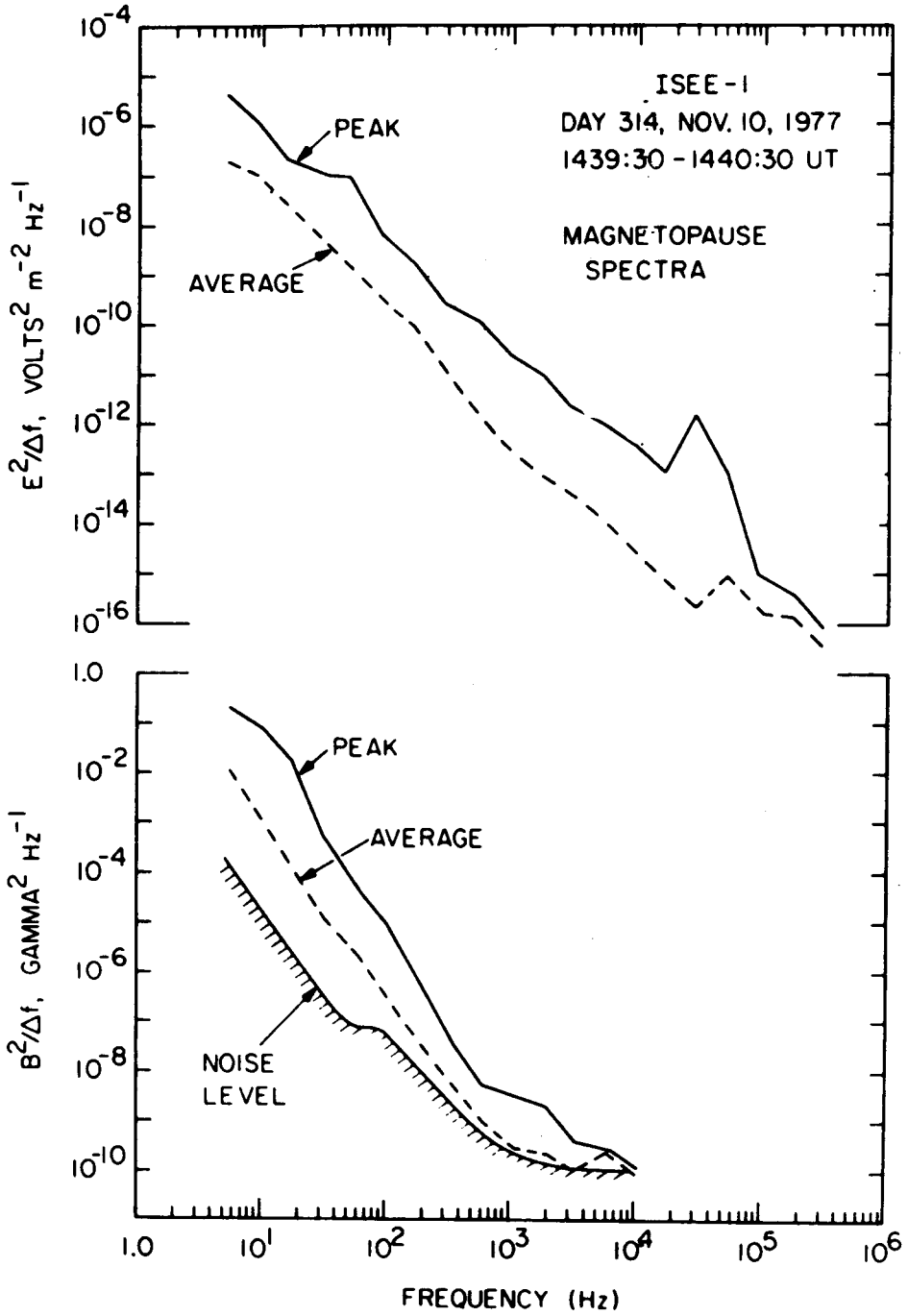

Figure 3. Shows the typical electric and magnetic field spectra of the enhanced plasma wave turbulence observed near the magnetopause. From Gurnett et al. (1979, Figure 10).

in the plasma wave characteristics at the magnetopause, in the boundary layer, and in flux transfer events (FTEs).

Gendrin (1983) examined the boundary layer magnetic wave spectrum at frequencies below 11 Hz during an unusual event when the magnetopause penetrated to the geosynchronous orbit of GEOS-2. He noticed that the wave intensity monotonically decreases with increasing frequency which is consistent with the previous ISEE results at higher frequencies. Rezeau et al. (1986) extended the work of Gendrin (1983) and made a comparison of magnetopause boundary waves and magnetosheath waves. Their results are shown in Figure 4. The upper panel is the magnetosheath spectrum for the 3 directional components whereas the lower panel is the same for the magnetopause boundary layer. The average magnetosheath spectrum is indicated by the dashed line in the lower panel for easy comparison. It is clearly seen that the boundary layer spectrum is enhanced above the magnetosheath spectrum (above 1 Hz) and has a similar frequency dependence.

LaBelle and Treumann (1988) analyzed the AMPTE/IRM plasma wave data and found that the spectrum of electric as well as magnetic fluctuations decreases with frequency. Figure 5 shows a comparison of many spacecraft observations for the magnetopause boundary layer waves as summarized by LaBelle and Treumann (1988). Although the figure contains measurements from different instruments sampling different latitudes, local times, and radial distances of the dayside magnetopause for different time-periods, together all of the measurements generally fit power law spectra for both electric and magnetic components. The various measurements all agree with one another, within an order of magnitude in power, which is the typical variation of the spectra from one event to another as found by Tsurutani et al. (1981).

Tsurutani et al. (1989) performed a statistical study of the broad-band plasma waves at the magnetopause using ISEE 1 plasma wave data. They detected enhanced wave intensities at 85% of all magnetopause crossings. Although wave amplitudes were highly variable from event to event, the wave spectra averaged over many passes were remarkably similar at dawn, noon and dusk local hours. They found that the average wave intensity has a little or no dependence on latitude ($-2°$ to $+25°$), magnetosheath field strength, or no magnetopause position. The waves were found to be slightly more intense during negative magnetosheath (interplanetary) B_z than during positive B_z.

Zhu et al. (1996) studied the ELF-VLF waves within the current layer of the dayside magnetopause using ISEE 1 data. Their database consists of 272 crossings of the dayside magnetopause from 1977 to 1979. They find a nearly linear relationship between the local magnetic shear angle and the wave amplitudes (both electric and magnetic components) as shown in Figure 6. The magnetic shear angle θ is calculated from the magnetic field vectors ($\mathbf{B_1}$, $\mathbf{B_2}$) from the magnetometer at the starting and ending times for a given magnetopause crossing, using the formula $\cos\theta = \mathbf{B_1} \cdot \mathbf{B_2}/(|\mathbf{B_1}||\mathbf{B_2}|)$. Assuming that the electric perturbations are perpendicular to the propagation direction (i.e., ambient magnetic field direction), they

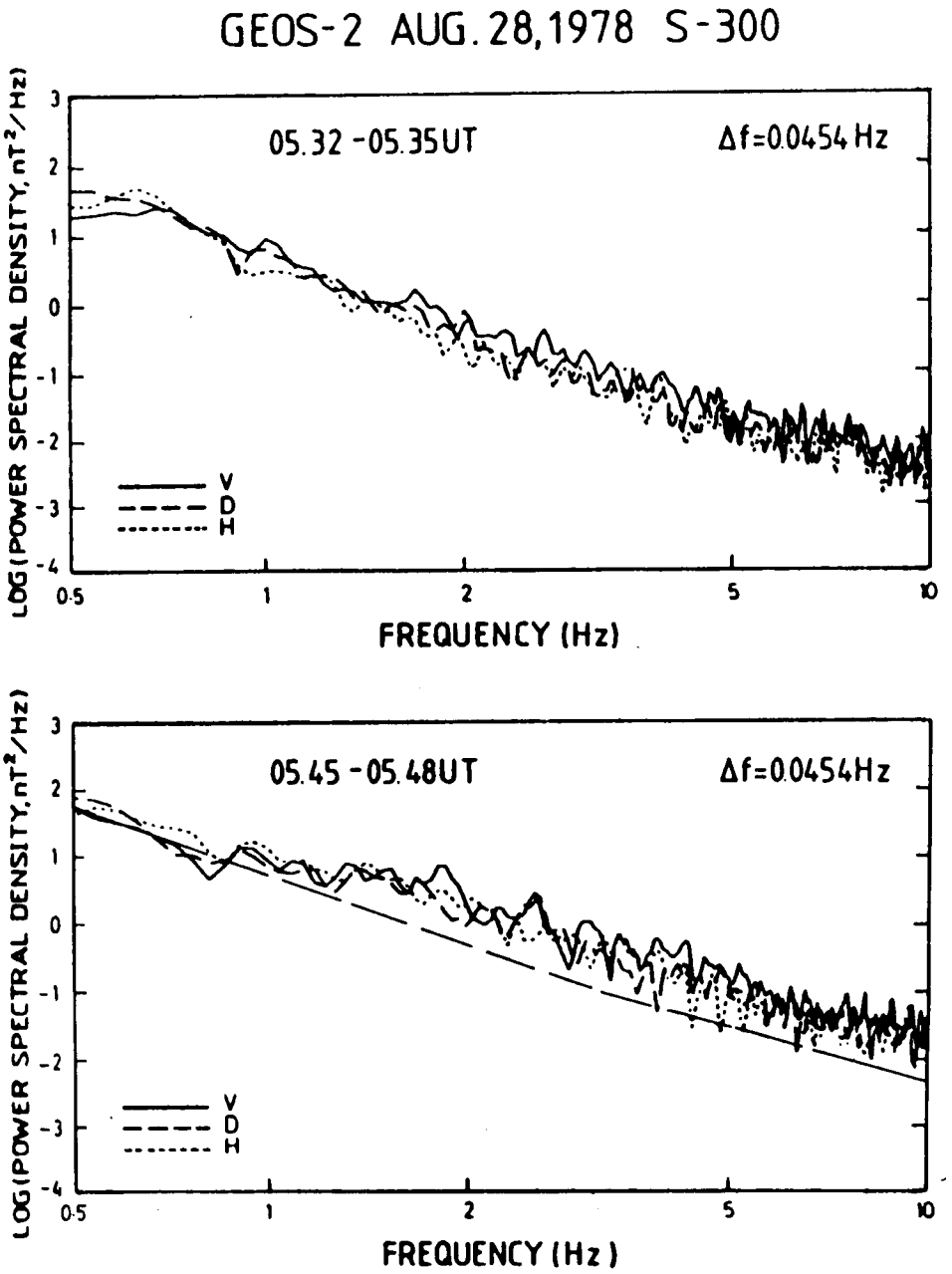

Figure 4. A comparison between the GEOS 2 Magnetopause BL magnetic wave spectrum (bottom) and the magnetosheath magnetic wave spectrum (top). The average magnetosheath spectrum is shown by the dashed line in the bottom panel. The BL wave spectrum is enhanced above the magnetosheath spectrum (except below 10 Hz). From Rezeau et al. (1986, Figure 3).

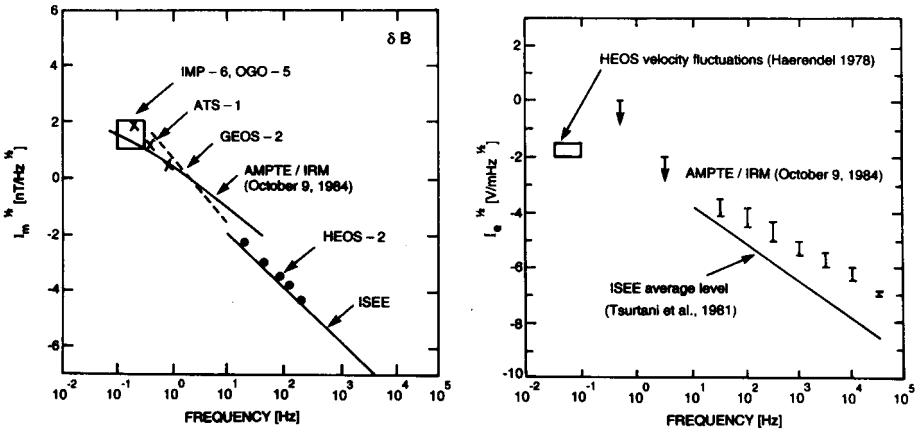

Figure 5. (a) The spectrum of magnetic fluctuations observed at the magnetopause from various different satellites. (b) The spectrum of electric fluctuations observed at the magnetopause from ISEE and from AMPTE/IRM. The IRM data come from a single day; the maximum value at the magnetopause is shown, along with the spectrum averaged over the magnetopause region. The IRM data from below 30 Hz are only upper limits on the wave amplitude. Also shown is the typical value of electric field fluctuations below 0.1 Hz corresponding to the velocity fluctuations reported from the HEOS satellite. From LaBelle and Treumann (1988, Figures 2 and 3).

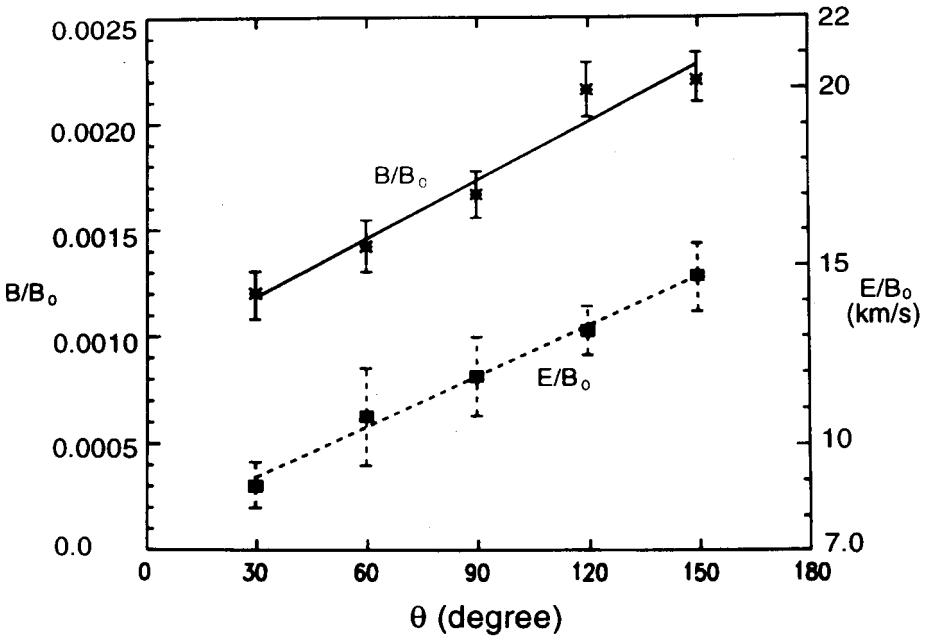

Figure 6. The amplitude of the normalized wave magnetic field (asterisks) and wave electric field (closed squares) as functions of local magnetic shear angle. Vertical bars indicate the deviations of the means. Solid and dashed lines are the linear fits to the wave magnetic and electric data, respectively. From Zhu et al. (1996, Figure 2).

estimated the phase velocity $v_{ph} = E(\omega)/B(\omega)$ for different frequency channels and obtained the dispersion relation for different shear angles. This dispersion relation had the characteristics of parallel propagating whistler modes, namely a rising tone and a cutoff at the electron cyclotron frequency. Based on the dispersion curves of the wave, they suggested that the waves are parallel propagating whistler modes. Recently, Song et al. (1998) have further extended the statistical study of Zhu et al. (1996). They found that most of the wave power in the current layer is in the magnetic fluctuations rather than the electric field fluctuations. Further, they found similar correlations between the wave power and the B_z component and magnetic shear angle θ as Tsurutani et al. (1989) and Zhu et al. (1996), respectively. In addition, they found a clear correlation between the broadband waves and the electron plasma beta, but no clear correlation between the wave amplitudes and the electron anisotropy. In a case study, they found the wave electric field to be polarized nearly perpendicular to the ambient magnetic field as found by Gurnett et al. (1979).

2.2. CROSS-FIELD DIFFUSION

The interaction of broadband plasma waves with the charged particles can cause scattering of the particles thereby changing particles' momenta and energies. Thus wave-particle interactions in a collisionless plasma can play a role similar to direct particle–particle collisions in a collisional plasma. The magnetopause boundary is more or less a collisionless plasma system. If there is no particle scattering by the waves, the magnetosheath ions are not expected to penetrate the boundary to a distance larger than a Larmor radius or so. Since the magnetopause thickness is generally much greater than an ion Larmor radius, the particle cross-field transport due to the wave-particle interaction has been invoked to explain the formation of the boundary layer.

2.2.1. *Resonant Wave Particle Interactions*

When a particle senses the wave Doppler-shifted to its cyclotron frequency (or its harmonics), it can interact strongly with the waves. The condition for this cyclotron resonance between the waves and the particles can be written as

$$\omega - k_{\|} v_{\|} = n\Omega, \tag{1}$$

where ω and $k_{\|}$ are the wave frequency and the parallel component of the wave vector $\mathbf{k}$, $v_{\|}$ is the parallel component of the particle velocity, $\Omega = qB_0/mc$ is the cyclotron frequency of the charged particle, B_0 is the magnetic field, q and m are particle charge and mass, respectively, c is the speed of light, and n is an integer equal 0, ± 1, ± 2, ... The $k_{\|} v_{\|}$ term is the Doppler shift effect due to the particle motion relative to the wave. The case of $n = 0$ corresponds to the Landau resonance. When condition (1) is satisfied, the waves and particles remain in phase, leading to energy and momentum exchange between them.

Tsurutani and Thorne (1982) have developed general expressions for cross-field diffusion of electrons and ions via resonant interaction with either electromagnetic or electrostatic waves. The cross-field diffusion rate due to the magnetic component of electromagnetic waves can be written as (Tsurutani and Thorne, 1982; Thorne aud Tsurutani, 1991; Tsurutani and Lakhina, 1997)

$$D_{\perp,B} = 2\eta \left(\frac{B}{B_0}\right)^2 D_{\max}, \tag{2}$$

where B is the amplitude of the wave magnetic field at the resonant frequency given by (1), η is a dimensionless scaling factor indicating what fraction of time the particles stay in resonance with the waves, and

$$D_{\max} = \frac{cmv_\perp^2}{2eB_0}, \tag{3}$$

is the Bohm diffusion rate (Bohm, 1949). Here, $v_\perp$ denotes the perpendicular velocity of the charged particles.

The cross-field diffusion rate due to the electrostatic waves is given by

$$D_{\perp,E} = 2\eta \left(\frac{E}{B_0}\right)^2 \left(\frac{c}{v}\right)^2 D_{\max}, \tag{4}$$

where E is the amplitude of the wave electric field at the resonant frequency given by (1), and v is the magnitude of the particle velocity.

Considering the boundary layer parameters, $B_0 \approx 50$ nT, $N \approx 20$ cm^{-3}, we note that protons of energies $\sim$1 keV will be in cyclotron resonance with the wave at $\omega/\Omega_p \sim 1$ is the proton cyclotron frequency), i.e., at frequencies close to 1 Hz. At these frequencies, the amplitude of the wave field is $B \approx 5$ nT (Gendrin, 1983; Rezeau et al., 1986), then from (2) we get $D_{\perp,B} = 260$ km^2 s^{-1} for 1.3 keV protons. On the other hand, 1 keV electrons will be resonant with the waves at frequency $\omega \sim \Omega_e/3$ (here Ω_e is the electron cyclotron frequency). As there is much less power at such high frequencies, therefore 1 keV electron diffusion due the cyclotron resonant process will be too small.

On the other hand, observations of Tsurutani et al. (1981) indicate the amplitude of broadband electrostatic waves to be $\sim$3 mV/m near Ω_p and $\sim 3 \times 10^{-3}$ mV/m near Ω_e. Then, from (4), the cross-field diffusion rates for the magnetosheath plasma ($\sim$1 keV protons and electrons) due to their cyclotron resonance with the electrostatic waves (Tsurutani and Thorne, 1982) is $D_{\perp,E} \approx 4 \times 10^2$ km^2 s^{-1} for $\sim$1 keV protons, and $D_{\perp,E} \approx 4 \times 10^{-4}$ km^2 s^{-1} for $\sim$1 keV electrons. Once again the electron diffusion is insignificant compared to the ion diffusion. It should be noted that theoretical models of either a viscous momentum transfer (Axford, 1964) or mass diffusion across the magnetopause (Sonnerup, 1980) require a kinematic viscosity or diffusion coefficient comparable to 10^3 km^2 s^{-1}

to account for the observed magnetopause boundary layer thickness. The cross-field diffusion rates for the magnetosheath ions due to resonant interaction with the electromagnetic or electrostatic waves are comparable to the value required to maintain the typical thickness of the boundary layer. Further, the broadband waves show significant variability in the power spectral densities for both magnetic and electric components (Gurnett et al., 1979; Tsurutani et al., 1981; Gendrin, 1983; LaBelle and Treumann, 1988; Tsurutani et al., 1989), which will result in substantially different rates of cross-field diffusion leading to observed variations in the thickness of the magnetopanse boundary layer.

It has been shown by Tsurutani et al. (1981) that the intense broadband waves in the magnetopause boundary layer will cause rapid isotropization both the electron and ion distributions. They found a strong correlation between intense broadband waves and 1–6 keV electrons and protons. The observed wave power was found to be sufficient to scatter the 1–6 keV electrons and protons near the limit of strong pitch angle diffusion. On using the measured spectrum of the ISEE 1 electrons and ions and integrating from 1 to 10 keV, the precipitated energy flux into the atmosphere was estimated to be 0.15 erg cm^{-2} s^{-1}. Taking into account the presence of enhanced ion fluxes at energies from 300 to 500 eV as observed by Tsurutani et al. (1989), the precipitated energy flux is increased to $\approx$1.0 erg cm^{-2} s^{-1}. These numbers are comparable to the dayside auroral energy input. Resonant cyclotron interactions between the waves and particles in the boundary layer can therefore provide a reasonable explanation for the nearly continuous presence of dayside aurora.

2.2.2. *Anomalous Diffusion from Plasma Instabilities*

Stochastic scattering of particles by microscopic plasma turbulence can lead to anomalous collision frequency, ν_{an}, in a collisionless plasma. This process is complementary to the resonant wave-particle interactions described above. The presence of a plasma density gradient perpendicular to a magnetic field gives rise to a cross-field current which can drive drift instabilities. Another source of free energy for the excitation of plasma instabilities is the field-aligned current (LaBelle and Treumann, 1988; Thorne and Tsurutani, 1991). The anomalous collision frequency due to plasma instabilities driven essentially by field-aligned currents is typically a fraction of the ion cyclotron frequency, i.e., $\nu_{an} \sim \Omega_p$ (Dum and Dupree, 1970; Treumann et al., 1991), whereas it can be substantially higher for the case of perpendicular current driven instabilities (LaBelle and Treumann, 1988; Thorne and Tsurutani, 1991). Anomalous collision frequencies can be used to estimate the cross-field diffusion coefficient (Ichimaru, 1972),

$$D_\perp = \frac{1}{2}\rho_e^2 \nu_{an} \left(1 + \frac{T_p}{T_e}\right), \tag{5}$$

where ρ_e is the electron gyroradius, and T_p, T_e are the respective proton and electron temperatures. LaBelle and Treumann (1988) have calculated anomalous colli-

sion frequencies for various perpendicular current driven instabilities by using the quasi-linear theory. A simple general approximate formula is

$$\nu_{an} \approx \frac{W}{m_e n V_D}\left(\frac{\gamma_m k_m}{\omega_m}\right), \tag{6}$$

where $W = \int W_k d^3k$ is the average wave energy density, n is the plasma density, V_D is the perpendicular current drift velocity, γ_m the maximum growth rate, ω_m and k_m are, respectively, wave frequency and the wave number corresponding to the maximum growth. The wave spectral energy density is given by

$$W_k = \left(\frac{\partial \omega \epsilon(\omega, k)}{\partial \omega}\right)\frac{1}{2}\epsilon_0 |\delta E_k|^2, \tag{7}$$

where $\epsilon(\omega, k)$ is the linear dielectric constant of the plasma for the wave mode under consideration, and δE_k is the linear wave amplitude. The above expressions are quite general, and applicable to a wider range of nonlinear waves if the dielectric constant and the amplitude are replaced by their nonlinear counterparts.

LaBelle and Treumann (1988) estimated anomalous diffusion coefficients for four plasma instabilities, namely, the modified two-stream instability (MTSI), the lower-hybrid drift instability (LHDI), the ion-acoustic instability, and the electron cyclotron drift instability (ECDI), based on their nonlinear saturation levels as predicted by the quasi-linear theory. They concluded that none of these four instabilities could provide adequate diffusion to maintain the boundary layer. Gary and Sgro (1990) and Thorne and Tsurutani (1991) pointed out an error in the estimation of the diffusion coefficient for the lower-hybrid instability in LaBelle and Treumann (1988). This was corrected by Treumann et al. (1991, 1995) who found that the resulting diffusion coefficient becomes large enough to explain the thickness of the magnetopause boundary layer. We will reproduce the correct expression for the anomalous collision frequency for the lower-hybrid instability.

The dielectric constant, $\epsilon(\omega, k)$, for the lower hybrid waves is given by (Lakhina and Sen, 1973; Davidson, 1978; Revathy and Lakhina, 1977)

$$\epsilon(\omega, k) = 1 + \frac{\omega_{LH}^2 \omega}{k^2 v_{tp}^2 (\omega - k V_D)} = 0, \tag{8}$$

where v_{tp} is the ion (proton) thermal speed and $\omega_{LH} = \omega_p/(1 + \omega_e^2/\Omega_e^2)^{1/2}$ is the lower-hybrid frequency. Here ω_e and ω_p are the electron and proton plasma frequencies, respectively. Then, from Equation (7) we get

$$W_k = \left(1 + \frac{\omega_e^2}{\Omega_e^2}\right)\left(1 + \frac{k^2 v_{tp}^2}{\omega_{LH}^2}\right)\frac{\epsilon_0}{2}|\delta E_k|^2, \tag{9}$$

Equation (8) yields the maximum growth rate $\gamma_m \approx (\sqrt{2\pi}/8)(V_D/v_{tp})^2 \omega_{LH}$ and corresponding $\omega_m \approx k_m V_D/2$. On substituting these in Equation (6), we obtain the

following expression for the anomalous collision frequency for the lower-hybrid instability,

$$\nu_{an}^{LH} = \left(\frac{\pi}{8}\right)^{\frac{1}{2}} \frac{m_p}{m_e} \left(1 + \frac{\omega_e^2}{\Omega_e^2}\right) \frac{W}{nT_p} \omega_{LH}. \tag{10}$$

Figure 7 shows the variation of the theoretical diffusion coefficients versus electric field power for four electrostatic modes considered by LaBelle and Treumann (1988) (this is a corrected version of their Figure 6). An average magnetic field strength of 50 nT, density n = 10 cm^{-3}, temperatures T_e = 25 eV, T_e = 1 keV have been assumed. The dots on each curve show the theoretically derived saturation levels of the respective instabilities. The vertical line is the upper limit of measured wave electric field intensity as deduced from the available satellite measurements of ISEE and AMPTE/IRM spacecraft. The horizontal dashed line gives the required Sonnerup diffusion limit. It is clear that the diffusion coefficient caused by the LHDI comes marginally close to the Sonnerup diffusion limit. However, the diffusion coefficients from the rest of the instabilities are too low to be significant for the maintenance of the low latitude boundary layer. Hence, the LHDI could, in principle, provide sufficiently high diffusion rates, based on observed wave power, to account for the existence of the LLBL under the conditions when reconnection in the vicinity of the subsolar stagnation point does not occur. It is interesting to note that all four electrostatic instabilities shown in Figure 7, and LHDI in particular, could provide the dissipation necessary to initiate reconnection at the magnetopause under southward, or inclined, IMF conditions. Cattell et al. (1995) concluded that the amplitudes of the magnetopause boundary layer waves were large enough to provide the dissipation required for reconnection to occur. Recently, Treumann (1997) has suggested that in the region of strong plasma wave activity Levy flight interactions can occur which may cause super-diffusive (of the order of or even greater than the Bohm diffusion) particle transport to populate the inner LLBL.

Gary and Sgro (1990) studied the lower hybrid drift instability at the magnetopause using a 2D hybrid computer simulation (particle ions, fluid electron with nonzero mass) code. On the other hand, Winske and Omidi (1995) and Winske et al. (1995) studied the magnetopause wave generation (at low-frequencies, i.e., $\omega \ll \Omega_p$, as well as at lower hybrid wave frequencies) and particle transport using a 2D hybrid code with particle ions and massless fluid electrons. The free energy source in all the above computer simulation studies was the density gradient. It was found that lower hybrid waves could give rise to diffusion comparable to the Bohm rate as required by Sonnerup (1980) to populate the low latitude boundary layer. However, the diffusion remained quite localized, meaning that diffusion per se leads only to some local relaxation of the gradients, and not to the formation of an extended boundary layer.

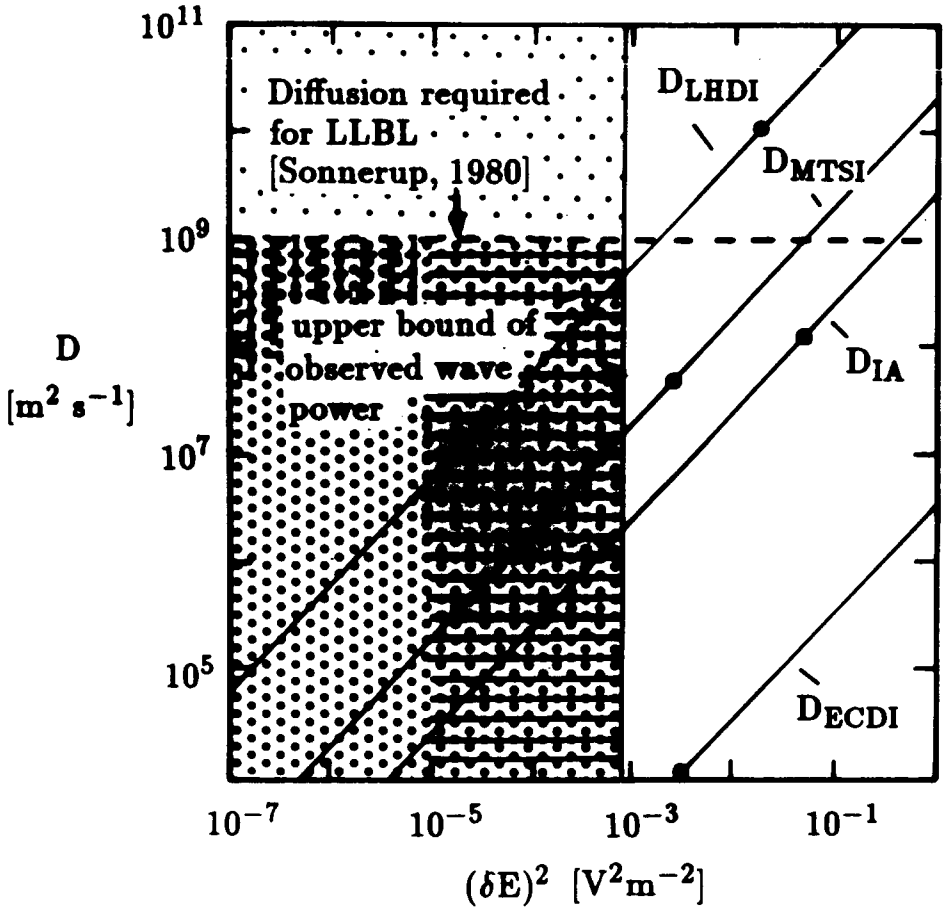

Figure 7. Different microscopic diffusion coefficients and their dependencies on the total electric wave intensity. The shaded region marks the range of the observed electric wave field strengths. The horizontal dashed line at $D = 10^9$ m^2 s^{-1} is the diffusion required to maintain the LLBL according to the theory of Sonnerup (1980). The dots indicate the diffusion coefficients according to theoretical saturation levels of the various instabilities. The double shaded regions mark the uncertainties in measured wave intensity and in the estimate of the diffusion coefficient. From Treumann et al. (1995, Figure 5).

3. Polar Cap Boundary Layer

3.1. WAVE OBSERVATION

Intense broadband plasma waves have been discovered, on the polar cap magnetic field lines which map to LLBL, by the Plasma Wave Instrument (PWI) (Gurnett et al., 1995) on the POLAR spacecraft. The wave character, e.g., spiky nature, frequency dependence, and intensity are quite similar to those of the low latitude boundary layer (LLBL) waves detected at and inside the low latitude dayside mag-

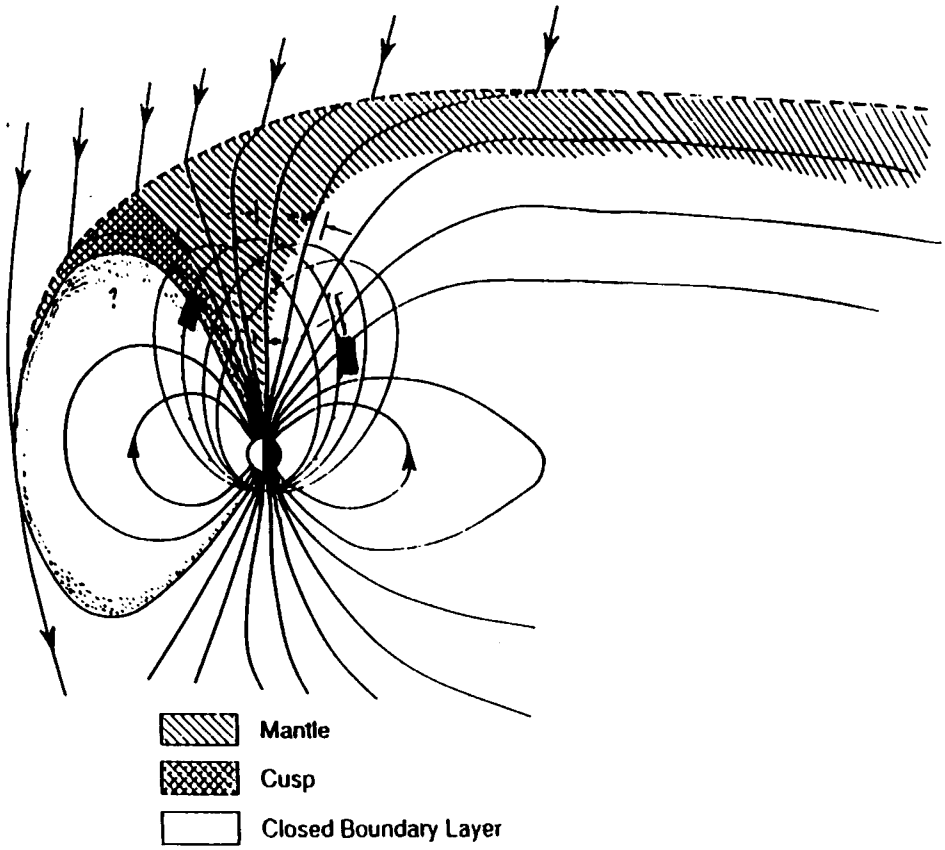

Figure 8. The POLAR orbit and the region of wave detection (solid bar) in the magnetosphere. POLAR has a perigee at $1.8R_E$ and apogee at $9R_E$. Waves on the field lines that map into the low latitude boundary layer (LLBL) are the topic of this study. From Tsurutani et al. (1998, Figure 1).

netopause (cf. Section 2). These waves, therefore, are called polar cap boundary layer (PCBL) waves (Tsurutani et al., 1998).

Figure 8 shows the POLAR orbit, which has an inclination of 86° with an apogee of $\sim 9R_E$ and perigee of $\sim 1.8R_E$ and covers the noon-midnight sector. Under ordinary circumstances the POLAR spacecraft does not intercept the magnetopause (Pickett et al., 1997) but, as shown in the figure, the spacecraft does cross field lines that map into the LLBL.

Plate 1 (taken from Plate 1 of Tsurutani et al., 1998) is a frequency-time spectrogram of the data obtained on April 7, 1996 from the POLAR Plasma Wave Multichannel Analyzer (MCA) (taken from Plate 1 of Tsurutani et al, 1998). This plot covers 24 hours as shown along the horizontal axis, and a frequency range of 5 Hz to 311 kHz, as shown along the vertical axis. The electric field power spectral density is plotted according to the color bar to the right of the spectrogram. The Universal Time (UT), radial distance from the center of the earth (R_E), magnetic

latitude (λ_M), magnetic local time (MLT), and approximate L-shell value, are indicated at the bottom of the plot. The wave regions are identified by referring to orbit information, and plasma wave data. Wave properties have been examined to identify the general modes.

The wave intervals of interest are indicated by two sets of arrows along the time axis, and are designated as "Dayside PCBL" and "Nightside PCBL" in Plate 1. These intervals of intense waves bound magnetic fields that map into the polar cap region. Both wave events occur in the northern hemisphere near the apogee. The dayside PCBL event occurs near 13.0 MLT and the other near 0.3 MLT, as the spacecraft orbit is in a near noon-midnight orientation. The PCBL waves are characterized by bursts of "turbulence" covering a broad frequency range extending from $f < 10^1$ to 2×10^4 Hz as shown in the MCA electric field spectrum of Plate 1. The magnetic field spectrum for these waves shows similar bursts (not shown). The region between the dayside PCBL and the nightside PCBL (about 0555 to 1450 UT) is identified as the northern polar cap. In this region there is typically a lack of strong signals although a few bursts of electrostatic noise are seen, as well as auroral hiss ($\sim$3 kHz) and auroral kilometric radiation ($\sim$100 kHz). The vertical lines found at about 1100 UT are instrument artifacts.

The statistical study, on the fractional amount of time that the waves were present from March 13 to August 31,1996 on the dayside (05 to18 GMT) near the POLAR apogee (comprising of 254 crossings), shows that enhanced waves were present 100% of the time near local noon with a slightly lower occurrence rate at dawn and dusk. The overall percentage of wave occurrence during this time interval was 96%.

The region of wave activity maps into a relatively narrow band of latitudes from 70° to 85° as seen in Figure 9a. This range gives the PCBL wave location. There is a trend for the PCBL waves to extend to slightly lower latitudes in both the dawn and dusk sides relative to the noon sector. The PCBL waves occur predominantly in the region with $L \geq 10$ as seen in Figure 9b. The wave location is slightly lower than cusp field lines.

The spectral density plots for both electric and magnetic fields are found to have rough power-law shapes. The intensities and spectral shapes vary from event-to-event, but generally follow a power law. The electric component has on average an $f^{-2.2}$ frequency dependence, and the wave frequency extends from $\sim 10^1$ Hz to $\sim 2 \times 10^4$ Hz, whereas the wave magnetic component has on average an $f^{-2.7}$ frequency dependence and appears to have an upper frequency cutoff at the electron cyclotron frequency. Moreover, the PCBL waves are found to be very bursty when seen in high time resolution wideband receiver (WBR) data. They last from tenths of seconds to tens of seconds, with the latter probably composed of several bursts occurring in succession or simultaneously (Tsurutani et al., 1998). Further, the average power spectra and the wave intensities for the electric and magnetic components for the events near the POLAR perigee in the southern hemisphere were found to be similar to those of the apogee events in the northern hemisphere.

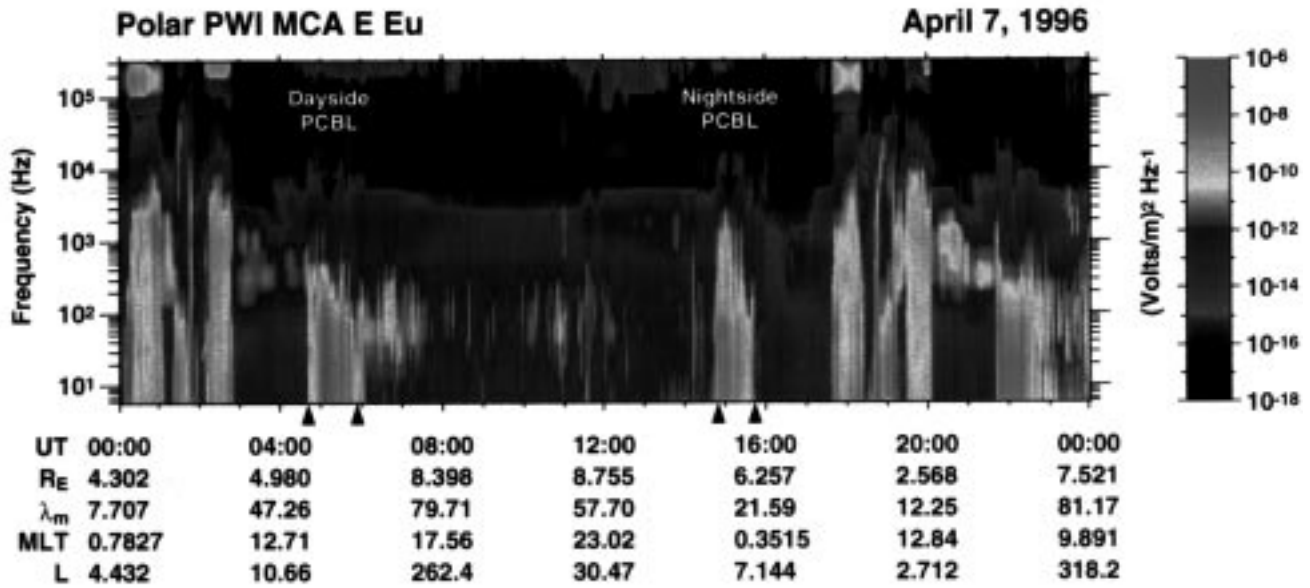

Plate 1. Spectrogram of wave electric field from $\sim 10^1$ to 10^4 Hz and above. The boundary layer waves are indicated. In between the two boundary layer (dayside and nightside) crossings is the polar cap (quiet wave region). From Tsurutani et al. (1998, Plate 1).

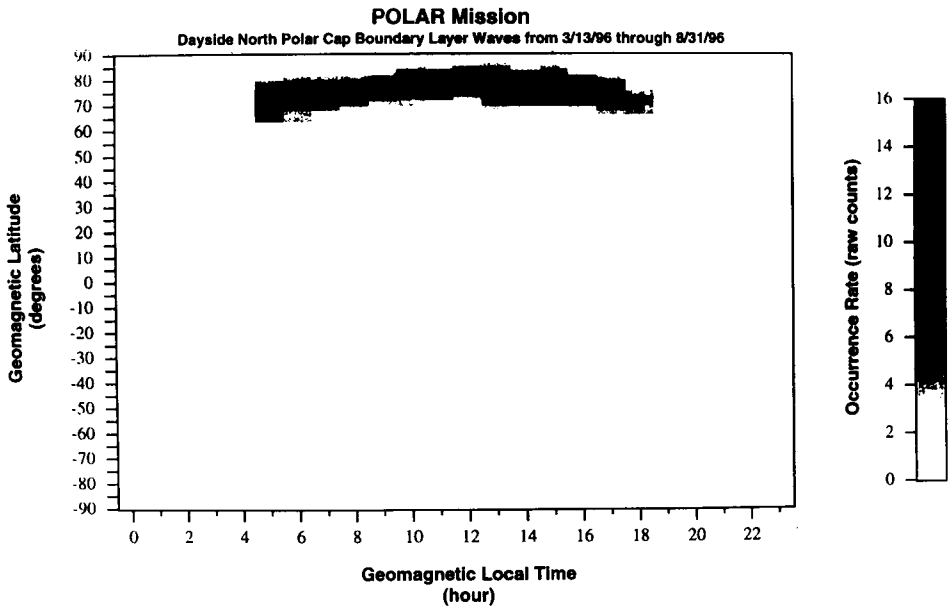

Figure 9. (a) The geomagnetic latitude of the footpoint of the B field line passing through the spacecraft versus local time (GMT). Regions of wave activity are primarily located on the field lines whose footpoint geomagnetic latitudes lie between 70°–80°.(b) L-value distribution of the PCBL waves versus GMT. The wave region is located for $L = 10$. From Tsurutani et al. (1998, Figure 4).

The electric and magnetic spectra of a typical event occurring near the apogee in the northern hemisphere on day 98, 1996 at 1302 MLT at 78.8° N invariant magnetic latitude is shown in Figures 10. For this event, the wave frequency of the electric component extends to $\sim 2 \times 10^4$ Hz (Figure 10a), and that of the wave magnetic component extends to 3×10^3 Hz (Figure 10b). Note that the electric component of the waves extends to frequencies above the electron cyclotron frequency. Although it appears that the wave magnetic component cuts off at the electron cyclotron frequency, f_{ce}, this is too close to the noise floor of the receiver to make any definite determination.

These broadband waves have both a magnetic and an electric component (cf. Figure 10). The B/E ratios lie in the range of 10 to 100. Thus, the wave phase velocities range from 3×10^3 to 3×10^4 km s^{-1}. Further, it has been noticed that the B/E amplitude ratio generally fits the parallel propagating whistler wave curve at the lowest frequencies ($f < 100$ Hz) and shows considerable departure from it at mid (10^2 Hz $< f < 10^3$ Hz) and high ($f > 10^3$ Hz) frequencies (Tsurutani et al., 1998). This indicates that there could be considerable (off-axis) refraction associated with the higher frequency components.

The broadband plasma waves are found to be well correlated with enhanced ion fluxes (H^+, O^+, He^+ and He^{++}) as detected by the toroidal imaging mass-angle spectrograph (TIMAS) (Shelley et al., 1995) experiment on POLAR. An example

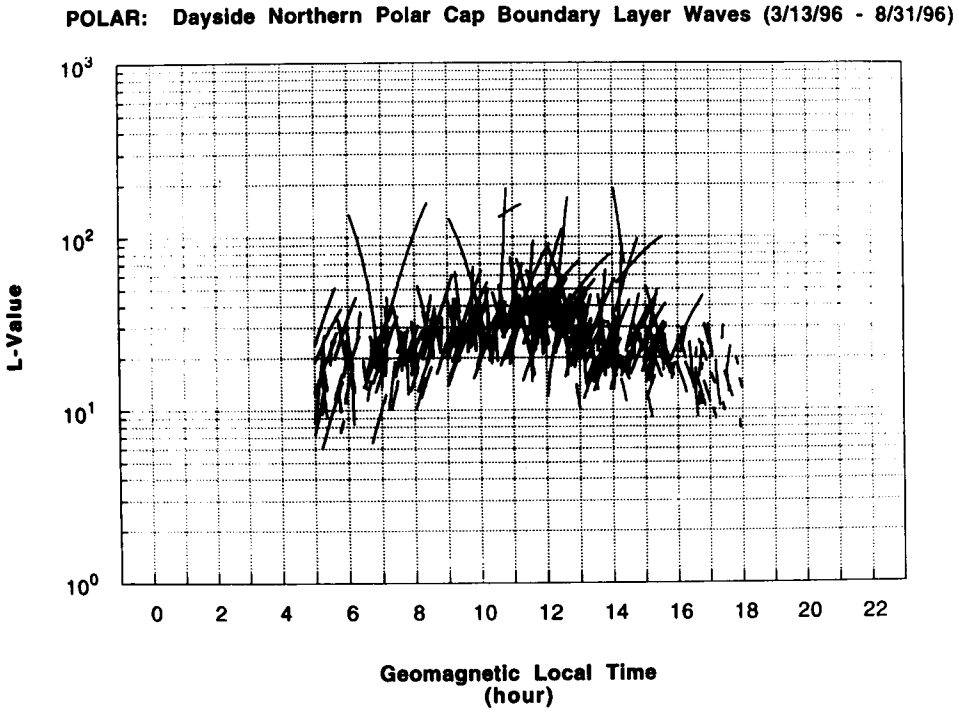

Figure 9b.

is shown in Plate 2 for April 7 (day 98), 1996. Prior to 0500 UT, the energy and angular distributions of ions reveal primarily hot quasi-isotropic ion populations characteristic of the dayside magnetosphere. The energy-latitude (time) dispersion in the H^+ and He^{++} populations beginning about 0505 and 0530 UT, are characteristic of the entry of magnetosheath plasma into the cusp or boundary layer. The region of most intense wave activity (0500 to 0515 UT) is associated with significant changes in the angular distributions in the upflowing O^+ ions. Specifically, in these regions, the upflowing, relatively low energy O^+ ions have angular distributions that are peaked at 50 to 70 degrees relative to the magnetic field direction. They have energies of a few hundred eV.

A systematic examination of the occurrence of these intense waves at the polar cap boundary at local times near dawn and dusk showed that, if upflowing O^+ ions are present at the time of these waves, the O^+ distribution has a characteristic conic angle (Tsurutani et al., 1998). However, it was also noted that there were intervals where intense waves were present, but no discernible upflowing O^+ ions were observed. The most probable mechanism for which the O^+ ions can gain significant energy transverse to the local magnetic field is through interactions with waves. Assuming that heating occurs primarily in the perpendicular direction, we can estimate the location of the region below the spacecraft. Because the magnetic field strength falls off roughly as r^{-3} and the first adiabatic invariant $mv_\perp^2/2B$ is

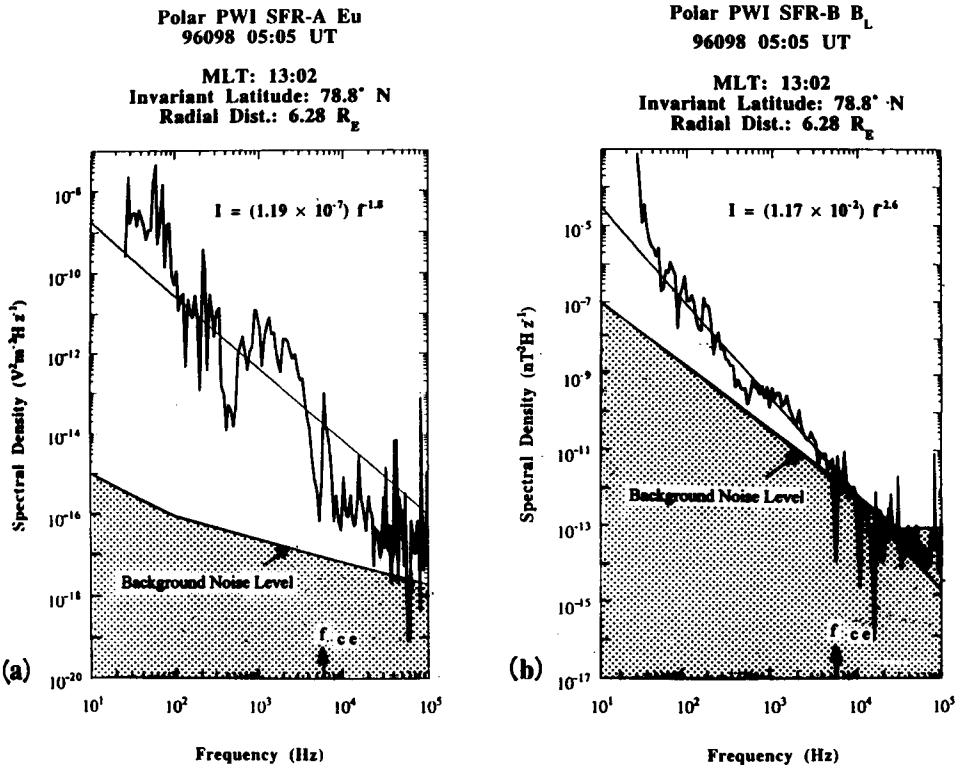

Figure 10. The electric field (a) and magnetic field (b) spectra for the events occurring on Day 098, 1996. The background noise is indicated. The electric component of the waves extend beyond the electron cyclotron frequency ($\sim 6 \times 10^3$ Hz). From Tsurutani et al. (1998, Figure 5).

conserved, we can estimate the maximum distance below the spacecraft where the transverse energy was possibly acquired. For conic angles of 50, 60, and 70 degrees at an altitude typical for these observations ($5.5R_E$), the maximum distances below the spacecraft where the transverse energy could be acquired are 0.9, 0.5, and 0.2 Earth Radii (R_E), respectively. These locations are quite close to the spacecraft, so the energization process is essentially a local one.

3.1.1. *Characteristics of PCBL Waves*

It is noticed (cf. Figure 8) that the PCBL waves occur on field lines that map into or close to the LLBL field lines. The wave characteristics are also quite similar to those of the LLBL waves. An inter-comparison between the POLAR wave power spectra and the LLBL waves as measured by ISEE-l and 2 and GEOS is given in Table 1. The GEOS event, which is much more intense than either ISEE-1 and -2 or POLAR wave intensities, is somewhat anomalous as it occurred during a magnetic storm when the magnetopause was pushed in to the spacecraft orbit ($6.6R_E$). It is possible that the extraordinarily high solar wind ram pressure and intense

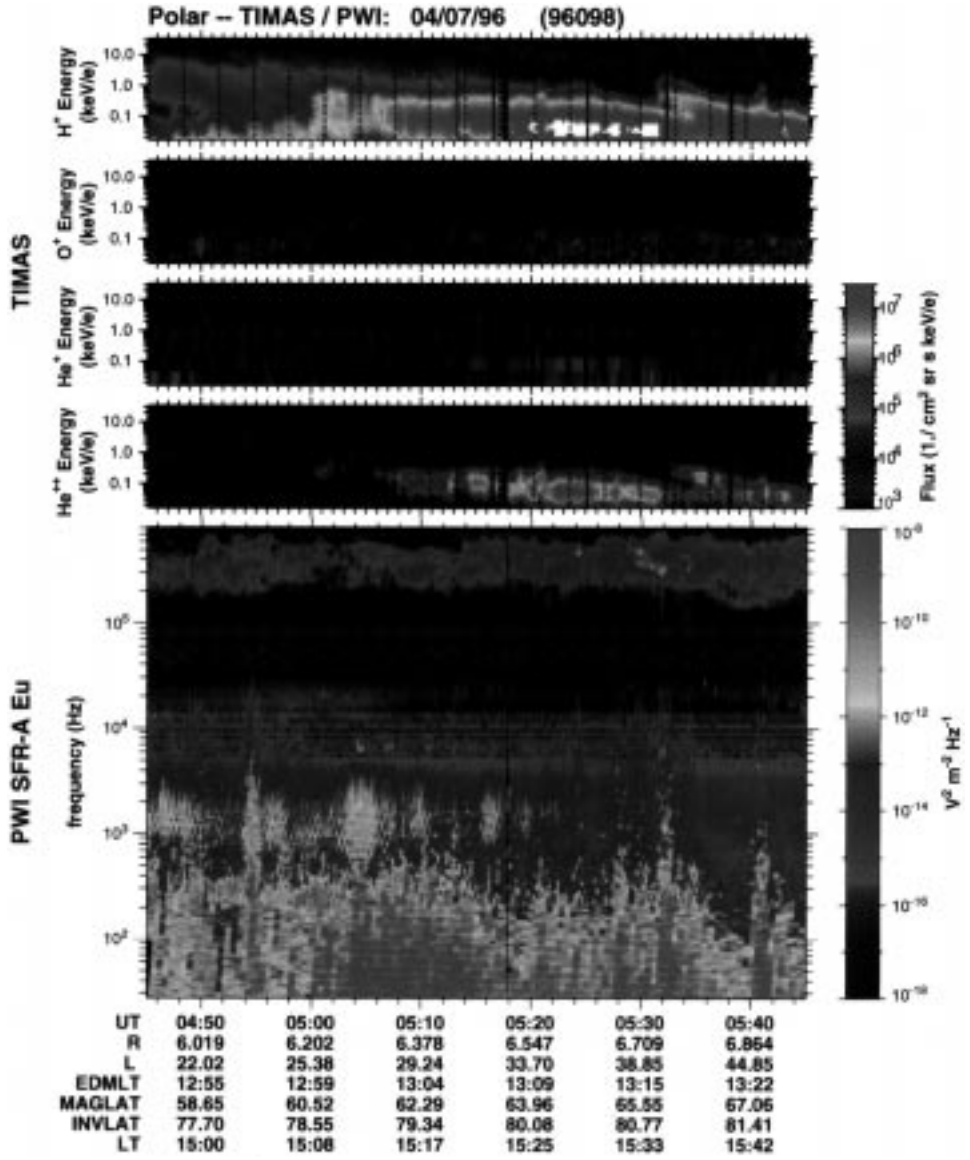

Plate 2. Spectrogram of the H^+, O^+, He^+ and He^{++} ion fluxes observed by the TIMAS experiment (top 4 panels) and the electric component of the PWI broadband plasma wave event (lower panel) on day 98, 1996. The values of eccentric dipole magnetic local time (ED MLT), magnetic latitude (MAGLAT), invariant latitude (INVLAT) and local time (LT) are also shown at the bottom of the Plate. From Tsurutani et al. (1998, Plate 3).

TABLE I

Comparison of broadband plasma wave properties in various boundary layers

Spacecraft	Location	Date	B $(\mathrm{nT})^2\ \mathrm{Hz}^{-1}$	E $V^2\ \mathrm{m}^{-2}\ \mathrm{Hz}^{-1}$
POLAR[1]	~ 7–$8R_E$ altitude	day 098, 1996	$1.17 \times 10^{-2} f^{-2.6}$	$1.19 \times 10^{-7} f^{-1.8}$
	$\sim 2R_E$ altitude	day 103, 1996	$1.34 \times 10^{-2.5} f^{-2.5}$	$1.22 \times 10^{-6} f^{-1.8}$
ISEE[2] 1	Earth's LLBL	day 314, 1977	$\sim f^{-3.3}$	$f^{-2.2}$
ISEE[3] 1, 2	Earth's LLBL	1977	$1.0 \times 10^{1} f^{-3.9}$	$3.0 \times 10^{-5} f^{-2.8}$
ISEE[4] 1, 2	Earth's LLBL	1977	$7.90 \times 10^{-2} f^{-2.9}$	$6.3 \times 10^{-6} f^{-2.2}$
GEOS[5] 2	Earth's LLBL	day 240, 1978	$3.60 \times 10^{1} f^{-2.6}$	$1.2 \times 10^{-6} f^{-2.6}$
ISEE[6] 1	Earth's LLBL	1977–1978	$3.0 \times 10^{-1} f^{-3.3}$	$6.0 \times 10^{-7} f^{-2}$

[1]Tsurutani et al. (1998).
[2]Gurnett et al. (1979).
[3]Tsurutani et al (1981).
[4]Anderson et al. (1982).
[5]Rezeau et al. (1989).
[6]Tsurutani et al. (1989).

southward interplanetary magnetic field B_s may have led to unusually high wave power during this event. Such LLBL wave intensity dependences on interplanetary parameters have been discussed by Tsurutani et al. (1989). Table 1 also lists a spectrum for day 103, 1996 for POLAR when it was near the southern hemisphere dayside perigee at $2R_E$. We note that the wave intensities are of the same order as the high altitude northern hemispherical events.

The main characteristics of the PCBL waves are summarized below:

1. The PCBL wave regions are located at 70° to 80° invariant magnetic latitude. This location is just below the cusp fields (75° to 85° latitude) and thus corresponds to LLBL field lines. The waves are present 96% of the time on the dayside (between 05 and 18 LT) at 6 to $8R_E$ in the POLAR orbit. The PCBL waves detected at low $2R_E$ altitudes are similar to those detected at high altitudes (6 to $8R_E$).
2. The emissions are bursty but, when averaged over longer time intervals, they fit a rough power law with an $f^{-2.2}$ dependence for E and $f^{-2.7}$ dependence for B waves, on average. The electric component extends from$\sim 10^1$ Hz to $\sim 2 \times 10^4$ Hz and the magnetic component from $\sim 10^1$ Hz to $\sim 5 \times 10^3$ Hz.
3. The waves have very similar intensities, spectral shapes and E and B dependences as the LLBL waves. The PCBL waves are similar to the broadband noise on auroral field lines (Gurnett and Frank, 1977; Gurnett et al., 1984) but, unlike the latter, the PCBL waves do not have any clear peaks at any frequency.
4. The B/E ratio is consistent with the parallel propagating whistler mode waves for the low frequency (10^1–10^2 Hz) component. However, the B/E ratio is

often higher at mid-(10^2–10^3 Hz) and high-(10^3–10^4 Hz) frequencies, which appears to be consistent with off-axis propagating waves.

5. The intense noon sector wave events are well correlated with enhanced fluxes of 10 to 200 eV H^+, He^{++} and O^+ ions.

Figure 11 shows a schematic of the magnetic field lines, the PCBL wave locations and the LLBL wave locations. Although to date such waves have been identified at only three regions along the field lines (PCBL, LLBL and near POLAR perigee), one can argue that the waves most likely exist along the entire length of the field lines provided that the field lines are "closed" and extend from one hemispherical ionosphere to the other. The PCBL wave field lines must be configured as indicated in Figure 11, where they map into the earth's ionosphere over a broad region of local times. Because the northern hemispherical waves are detected at only 6 to $8R_E$ from the Earth at relatively strong fields, the chance that they map into the cusp region is highly improbable. Russell (personal communication 1997) has reported that the POLAR magnetometer (statistically) detects cusp field lines at slightly higher latitudes and that the cusp only extends 2 hours from local noon at POLAR altitudes. The three point intensity (LLBL, POLAR near-apogee, POLAR near-perigee) measurements give strong constraints on the wave source location. An ionospheric source can be ruled out because if wave generation occurs in the ionosphere, upward wave propagation would lead to wave intensity decreases (from POLAR perigee to LLBL location) by orders of magnitude due to flux tube expansion alone. Wave damping and scattering would decrease intensities further. Other possibilities that have been discussed in the literature are that magnetosheath magnetosonic waves couple into LLBL Alfvén waves (Johnson and Cheng, 1997) or that magnetosheath waves are amplified at the magnetopause and propagate down the magnetic field lines (Belmont et al., 1995). If this were the case, then one would expect waves to be located primarily at noon with little or no waves present at the PCBL dawn and dusk flanks. There is some evidence for this (cf. Figure 3 of Tsurutani et al., 1998); however it is only slight. Moreover, this wave-coupling mechanism would work only for ultra-low-frequency (ULF) waves which are much below the PCBL broadband plasma wave frequencies. The most likely scenario is wave generation by a local source of free energy existing along field lines. Two possible sources are field-aligned currents and density gradients (Drake et al., 1994a, b; Lakhina et al., 1997; Lakhina and Tsurutani, 1999).

4. Generation Mechanisms

The plasma waves observed in the low-latitude boundary layer and in the PCBL are broadband with no obvious spectral peaks which could be used to identify the plasma instabilities exciting these modes. Further, the boundary layers are the site of many free energy sources existing simultaneously, so it is not an easy task to identify which free energy source could be dominant for a given event. The

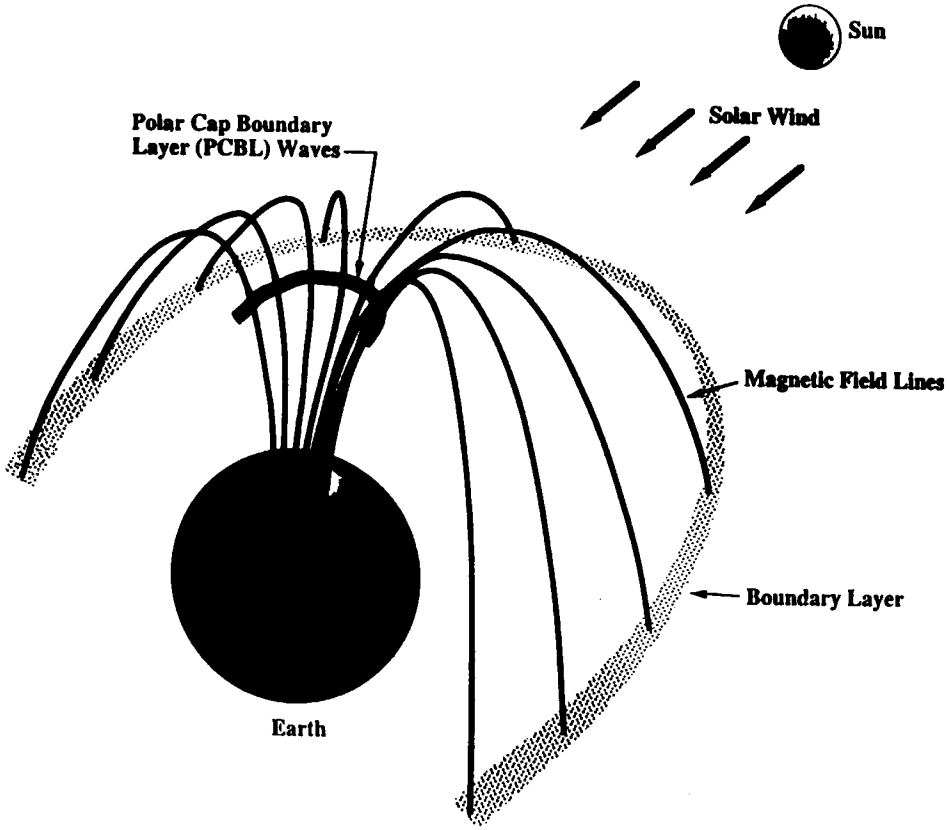

Figure 11. A northern polar view of the mapping of polar cap boundary layer (PCBL) waves to the low latitude boundary layer (LLBL). From Tsurutani et al. (1998, Figure 8).

changing interplanetary conditions can further complicate the identification of the free energy source and relevant plasma instability driven by it. There are density, temperature, velocity and magnetic field gradients present at both LLBL and PCBL. These gradients could act as sources of free energy for wave generation. In addition, the boundary layers can support strong currents, particle beams, and anisotropic velocity space distributions.

A number of possible wave modes have been discussed in the literature for the BL waves. We will mention only some of the important modes briefly here.

4.1. LOWER HYBRID DRIFT INSTABILITY

The lower hybrid drift instability (LHDI) is driven essentially by the density gradients present in the boundary layer (Gary and Eastman, 1979; Huba et al., 1981). Gary and Sgro (1990), Winske and Omidi (1995) and Winske et al. (1995) studied the lower hybrid drift instability at the magnetopanse using a 2D hybrid computer simulation (particle ions, fluid electrons) code. The LHDI is basically an

electrostatic instability, and the waves are generated near the lower hybrid wave frequencies. These short wavelength waves could be Doppler shifted to form a broadband spectrum. This instability is a plausible candidate that can give rise to cross-field plasma transport.

4.2. MODIFIED TWO STREAM INSTABILITY

The modified two-stream instability (MTSI) is very similar to the LHDI and is driven by the presence of both density gradient and the currents (McBride et al., 1972; Lakhina and Sen, 1973; Revathy and Lakhina, 1977; Papadopoulos, 1979). Like the lower hybrid drift instability, this instability also leads to anomalous resistivity and cross-field particle diffusion. The density gradients, whether weak or strong, are always present in the boundary layers. These density gradients can lead to the excitation of low-frequency electromagnetic drift Alfvén wave or drift kinetic Alfvén wave instabilities in the boundary layers (Chmyrev et al., 1988; Lakhina et al., 1993; Johnson and Cheng, 1997). The frequencies generated by this mechanism fall in the range of ULF frequencies, and therefore the mechanism is suitable for explaining the lowest frequencies of the broadband wave spectrum.

4.3. LOSS CONE INSTABILITY

Electromagnetic waves of whistler-type can be generated by the electron loss cone instability which is driven by velocity space gradients (Kennel and Petschek, 1966). However, the required anisotropy in the electron distribution functions has not been observed for the case of LLBL waves (Gurnett et al., 1979). Another problem with this mechanism is to explain the broadband nature of the BL waves.

4.4. ION-ACOUSTIC INSTABILITY

This is the current-driven electrostatic instability. The instability is excited when the field-aligned drift velocity exceeds the ion-acoustic speed (Kindel and Kennel, 1971). This instability has been suggested to explain the generation of broadband electrostatic noise (BEN) in the magnetotail (Akimoto and Omidi, 1986). However, this instability requires $T_e \gg T_i$, a condition which is not met in the boundary layers. This makes the ion-acoustic instability an unlikely mechanism for the BL waves.

4.5. ION CYCLOTRON INSTABILITY

This is an electrostatic instability propagating nearly perpendicular to $\mathbf{B}_0$, and is driven by the field-aligned currents (Ashour-Abdalla and Thorne, 1977, 1978; Swift, 1977). The instability can occur even when $T_e \sim T_i$. Since sufficiently strong field-aligned currents are expected to be present in the Earth's BLs as well as in PCBL, this instability is a good candidate for the generation of BL waves.

The main problem with this instability is that one requires very high harmonics to explain the observed broadband spectrum.

4.6. Electrostatic electron cyclotron instability

This instability excites electrostatic emissions with frequencies above the electron cyclotron frequency, e.g., $(n+\frac{1}{2})f_{ce}$ (n being the harmonic number) emission. The instability requires the presence of at least two electron populations, namely, hot, weak loss-cone component, and a cold dense component. The hot electron component, which contains regions of velocity space where $\partial f/\partial v_\perp > 0$, provides the free energy for the instability, while the cold electron component helps destabilization and controls the dispersion of the waves. The instability is strongest in the vicinity of the cold plasma upper-hybrid frequency, f_{uhc} (Young et al., 1973; Ashour-Abdalla and Kennel, 1978; Rönnmark et al., 1978; Kennel and Ashour-Abdalla, 1982). The broadband nature of the waves can be explained by assuming excitation of many harmonics and strong Doppler shifts. The main difficulty with this mechanism is that it is difficult to explain the strongest wave power at low-frequencies (i.e., $f \sim f_{ci}$ or smaller).

4.7. Velocity shear instabilities

The presence of velocity shear in the boundary layer can excite the Kelvin–Helmholtz (KH) instability (Chandrasekhar, 1961). The KH instability generates low-frequency ($f \ll f_{ci}$), long-wavelength (i.e., $\lambda \gg \rho_i$, where λ and ρ_i are, respectively, the wavelength of the mode and the ion Larmor radius) waves, and it can produce high anomalous viscosity at the magnetopause BL (D'Angelo, 1973; Miura, 1987; Lakhina, 1994; Ganguli et al., 1994). However, in the presence of field-aligned ion beams with sufficiently strong velocity shear, a short wavelength kinetic KH instability having frequencies near ion cyclotron harmonics ($f \approx nf_{ci}$, where n is the harmonic number) can be excited (Lakhina, 1987).

Similarly, the gradient of the field-aligned current can excite an electrostatic current convective instability and a whistler instability (Drake et al., 1994b; Drake, 1995; Zhu et al., 1996).

The mechanism of current convective instability demands that the thickness of the magnetopause current layer, L, be very narrow such that $L < \delta_e$, where $\delta_e = c/\omega_{pe}$ (c and ω_{pe} are the speed of light and the electron plasma frequency, respectively) is the electron skin depth. The whistler instability on the other hand requires that $L < \delta_i$, where $\delta_i = c/\omega_{pi}$ is the ion skin depth. The observed thickness of the magnetopause is typically several times the ion skin depth. Although all these mechanisms can explain the strongest wave power at the lowest frequencies, they suffer from a common drawback as to how to cascade the power to VLF frequencies.

4.8. ION BEAM INSTABILITIES

The presence of ion beams in the boundary layer can give rise to various type of electromagnetic and electrostatic instabilities. The electromagnetic instabilities generate long-wavelength, low-frequency waves, which can be either resonant or nonresonant with the beam ions (Gary et al., 1984; Verheest and Lakhina, 1991, 1993). On the other hand, the electrostatic modes generate modes at somewhat higher frequencies and shorter wavelengths as compared to the electromagnetic modes (Lakhina, 1993). In these mechanisms, the wave power is usually concentrated towards the lowest frequencies. To explain the wave power at higher frequency, one has to invoke strong Doppler shifts as well as some cascade mechanism.

4.9. COUPLED VELOCITY SHEAR-LOWER HYBRID INSTABILITIES MODEL

All the models described above consider only one free energy source at a time. As mentioned above, several free energy sources could simultaneously be present in the boundary layers. This could couple various modes excited by different free energy sources, or even lead to some new modes altogether. Lakhina and Tsurutani (1999) have presented a linear theory for the generation of broadband PCBL plasma waves. The theory is based on two-fluid equations, is fully electromagnetic and takes into account the free energy available due to the presence of field-aligned currents, and gradients in the currents, the plasma densities and the magnetic fields. The dispersion relation generalizes the dispersion relations for several plasma modes, including the lower hybrid (Gary and Eastman, 1979), the modified-two stream instability (Lakhina and Sen, 1973), beam modes (Dum, 1989; Lakhina, 1993), current convective and whistler instabilities (Drake et al., 1994a, Drake, 1995). In general, the beam driven modes, the current convective and the lower hybrid drift modes are coupled, and the dispersion relation has to be solved numerically. It is found that density gradients tend to stabilize both the current convective and the whistler instabilities, at the same time these modes develop real frequencies. On the other hand, sharp density gradients can lead to the excitation of a lower hybrid drift instability when the hot ions are present in the boundary layer.

Figure 12 shows the dispersion relation for the coupled lower hybrid and current convective modes in a hot plasma. Here, the equilibrium magnetic field varies along the x-direction, the direction of inhomogeneity, and is directed along the z axis, i.e., $\mathbf{B}_0 = B_0(x)\mathbf{z}$. There is a finite field-aligned current carried by electrons streaming with a nonuniform velocity $\mathbf{V}_0(x)$ relative to ions. The waves are propagating obliquely to the ambient magnetic field in the y–z plane, i.e., the wave vector $\mathbf{k}$ can be written as $\mathbf{k} = k_z\mathbf{z} + k_y\mathbf{y}$. The velocity shear is defined as $S = (\mathrm{d}V_0/\mathrm{d}x)\omega_{ce}^{-1}$, $\beta_i = 8\pi n_0 T_i/B_0^2$ is the ratio of ion pressure to the magnetic field pressure, and $a = k_y V_{ti}/\omega_{ci}$ is the perpendicular wave number normalized by the ion gyroradius $\rho_i = V_{ti}/\omega_{ci}$. Further, $\kappa_n = \mathrm{d}\ln n_0/\mathrm{d}x$ is the inverse of equilibrium density gradient, and $\kappa_B = \mathrm{d}\ln B_0/\mathrm{d}x$ is the inverse of the ambient magnetic field gradient.

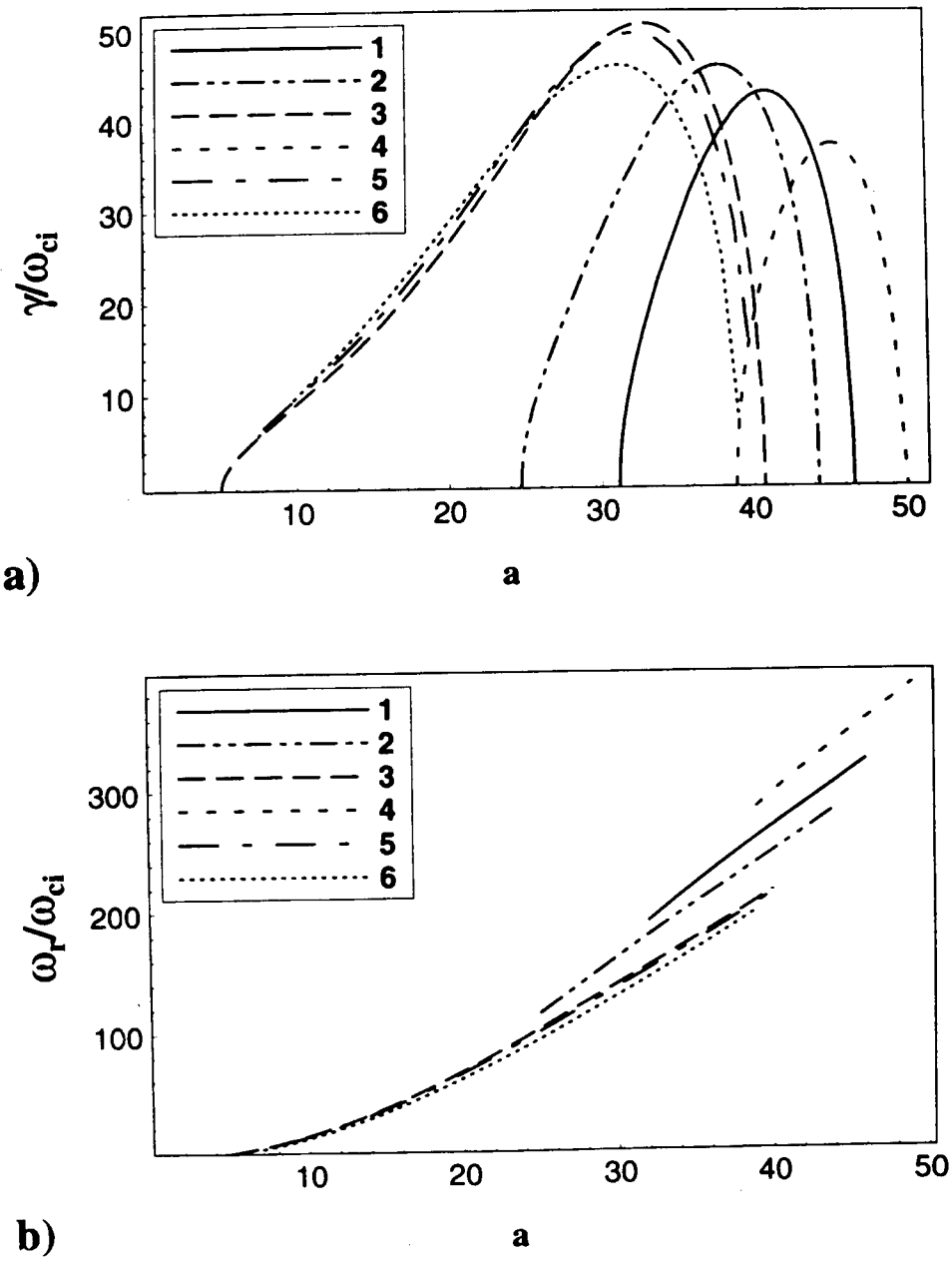

Figure 12. Variation of normalized growth rate, γ/ω_{ci}, (upper panel) and normalized real frequency, ω_r/ω_{ci}, (lower panel) versus normalized wavenumber $a = k_y V_{ti}/\omega_{ci}$ for the coupled lower hybrid drift and current convective instability for the case of hot plasma with $\omega_{pe}/\omega_{ce} = 10.0$, $V_0 = 0$, and $\kappa_n/k_y = 0.1$. The curves 1, 2, and 3 are for $\beta_i = 0.0$, $k_z/k_y = -0.1$ and $S = (1/\omega_{ce})(\mathrm{d}V_0/\mathrm{d}x)$ = 0.0, 0.05, and 0.1, respectively. The curve 4 is for $\beta_i = 0.0$, S = 0.1, and $k_z/k_y = 0.1$. The curves 4 and 5 are for S = 0.1, $k_z/k_y = -0.1$ and $\beta_i = 0.05$ and 0.2, respectively. From Lakhina et al. (1997, Figure 6).

The coupled lower hybrid-current convective modes tend to be stabilized by an increase in the value of β_i (cf. curves 1, 5 and 6). The velocity shear S can have either a destabilizing or a stabilizing effect on these modes depending on the sign of the parameter k_z/k_y (cf. curves 1, 2, 3 and 4).

4.9.1. *Physical mechanism of the instability*

In the model by Lakhina and Tsurutani (1999), the density gradients tend to reduce the growth rate of the current convective and whistler instabilities. Since the density gradients provide a free energy source, normally one would expect the density gradients to increase the growth rate of the instabilities, for example, the modified two-stream and lower hybrid instabilities discussed above. However, in general, the effect of the density gradients, or any other free energy source, could be destabilizing for some modes and stabilizing for the others, depending upon the nature of the excited modes. It has been shown that density gradients tend to stabilize the Kelvin–Helinholtz instability which is driven by a velocity shear (D'Angelo, 1965; Rome and Briggs, 1972; Catto et al., 1973; Huba, 1981). Both the current convective and whistler modes, like the Kelvin–Helmholtz modes, are driven by a parallel velocity shear, and therefore their basic nature is expected to be similar to the latter. The physical mechanism of the velocity shear instability is explained in Figure 13. In a uniform plasma, a perturbation electric field causes the electron to $\mathbf{E} \times \mathbf{B}$ drift along x. In the presence of velocity gradients, the convection of the electron flow v_z brings regions of different parallel flow to the same magnetic field line (Drake et al., 1994a). The resultant bunching of electrons along this magnetic field line produces an electric field which reinforces the initial perturbation, thereby producing an instability. The presence of a local density gradient would alter the nature of the bunching process. It introduces perturbations in the electron density, which in turn produce perturbations in the parallel electron velocity which are in the opposite direction to the perturbations in v_z produced by the velocity gradients. Thus, the presence of density gradients tend to debunch the electrons along **B** and reduce growth of the velocity shear modes.

4.9.2. *Generation of PCBL Waves*

The typical real frequencies generated by the Lakhina and Tsurutani (1999) model are in the range of 10 to $400\omega_{ci}$ with the parameter a lying in the range of $5 \leqslant a \leqslant 50$. The plasma density at the POLAR apogee is highly variable. The density can vary from 0.05 to 10 particles cm^{-3}, or even more. Similarly, the currents can vary considerably during a given pass, and from one pass to the next. There are indications of very sharp current gradients (as narrow as $3\rho_e$, where ρ_e the electron gyroradius) in the cusp region. For the PCBL region, typically ω_{ci} is ~4–5 Hz (Russell et al., 1995, Tsurutani et al., 1998), $T_i \sim 200$ eV, and $\beta_i \leqslant 0.05$. The typical ion gyroradius would be $\rho_i \approx 5.0$ km. A range of parameters need to be considered to reflect the variability in the observed plasma and field quantities near the POLAR apogee. For example, the values of κ_n/k_y = (0.01–0.2) corres-

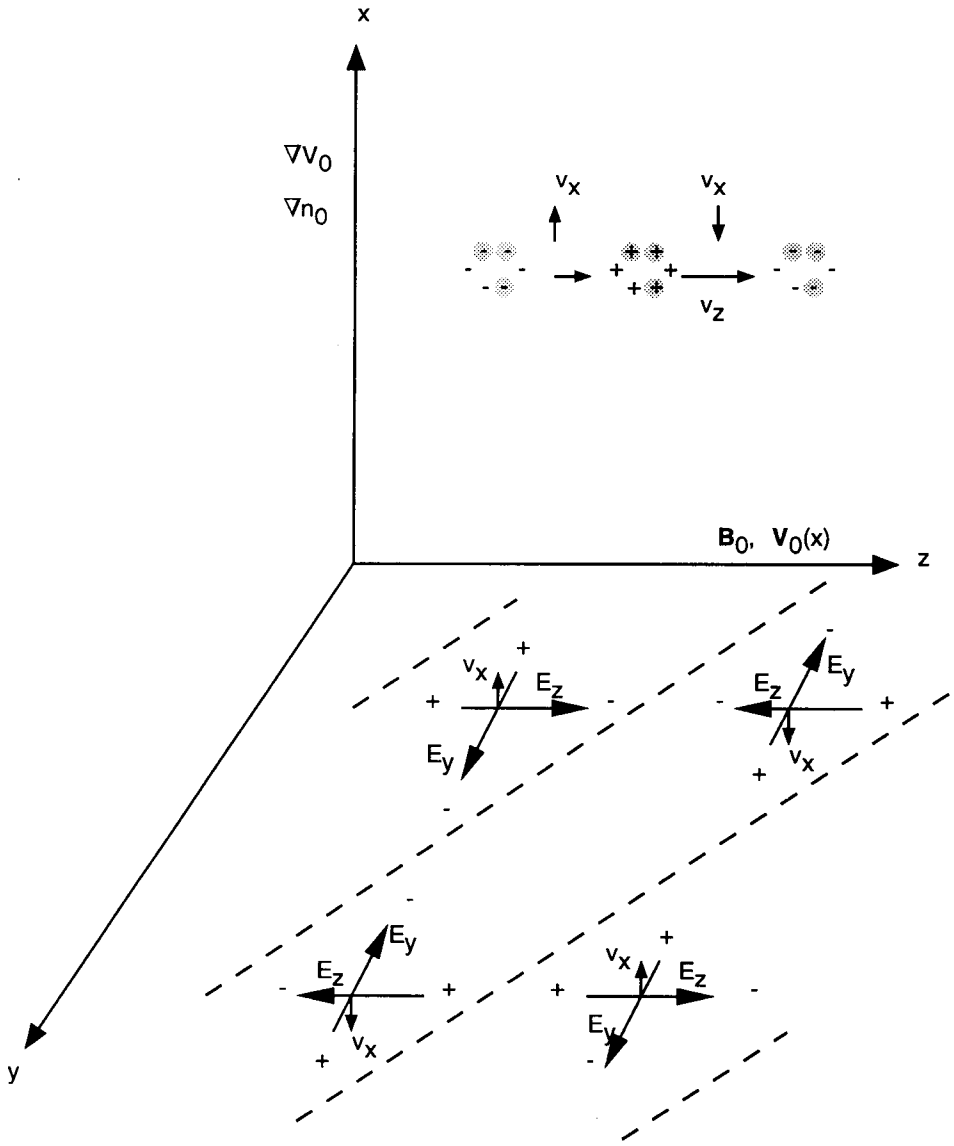

Figure 13. Schematics of the physical mechanism of the velocity shear instability. The equilibrium magnetic field $\mathbf{B}_0$ is taken along the z axis. The equilibrium electrons flow $\mathbf{V}_0$ is parallel to the magnetic field $\mathbf{B}_0$. The parallel electron velocity gradients ∇V_0, which derives the instability, and the density gradient ∇n_0 are in the x direction. The assumed form of the perturbing field $\mathbf{E} = E_z\mathbf{z} + E_y\mathbf{y}$ is shown in the y–z plane. The convection of the electron flow v_z brings regions of different parallel flow to the same magnetic field line. The resultant bunching of electrons along this magnetic field line (shown in the x–z plane) produces an electric field which reinforces the initial perturbation, thereby producing an instability. The presence of density gradients tends to debunch the electrons along **B** (i.e., the particles shown as shaded in the x–z plane are removed), thereby reducing growth of the velocity shear modes. From Lakhina et al. (1997, Figure 7).

pond to density gradient scale lengths of $L_n \simeq$ (0.5 to 100) km, S = (0.01–0.3) translate to velocity gradients of $L_v \simeq$ (0.5–20) km on assuming typical energies of 10 eV for the field-aligned electron beams. In view of the above parameters, the plasma rest frame frequencies of the excited modes would be of the order of 40 to 2000 Hz. In the satellite frame of reference, this frequency range would be broadened due to Doppler shifts and this could explain the observed frequency range of the broadband waves. The typical perpendicular wavelengths associated with the unstable modes would be $\lambda_\perp = 2\pi/k_y \simeq$ (0.6–6.0) km. Since the model describes coupled electrostatic and electromagnetic modes, the waves excited by the instabilities would have a mixture of electrostatic and electromagnetic modes, thus, naturally explaining an important characteristic of the PCBL waves.

5. Conclusion

We have described the characteristics of the broadband plasma waves observed in the Earth's magnetopause BL and in the PCBL. The waves are spiky signals spanning a broad frequency range from less than the ion cyclotron frequency to probably greater than electron cyclotron frequency. Both the electric and magnetic components of the wave have on the average a rough power law spectral shape. The frequency dependence and the amplitude ratio B/E suggest that the waves are most likely a mixture of electrostatic and electromagnetic modes. Various mechanisms for the generation of BL waves are discussed.

It appears that the broadband plasma waves discussed here are ubiquitous to the plasma flow boundary layers. It is interesting to point out that magnetotail (Scarf et al., 1972; Gurnett et al., 1976; Cattell et al., 1986; Gurnett and Frank, 1977; Matsumoto et al., 1994; Kojima et al., 1997), on cusp and auroral field lines (Gurnett and Frank, 1977, 1978; Pottelette et al., 1990; Dubouloz et al., 1991; Ergun et al., 1998), and in the magnetosheath (Anderson et al., 1982). The magnetotail BEN emissions are correlated with ion and electron beams, whereas auroral region BEN emissions are usually associated with ion conics and field-aligned electron beams. Dubouloz et al. (1991) have proposed a generation mechanism for auroral field line BEN in terms of electron acoustic solitons. The waveform observations by the plasma wave instrument on board the Geotail spacecraft have shown that BEN consists of a series of bipolar solitary pulses (Matsumoto et al., 1994). The broadness of the BEN frequency spectra arises from the solitary waveforms. A likely generation mechanism for BEN is based on the nonlinear evolution of the electron beam instabilities leading to the formation of the isolated Bernstein–Greene–Kruskal (BGK) potential structures which reproduce well the observed electrostatic solitary waveforms (Omura et al., 1996; Kojima et al., 1997). The mechanisms discussed by Matsumoto et al. (1994) and Dubouloz et al. (1991) predict negatively charged structures whereas the POLAR (Franz et al., 1998) as well as FAST (Ergun et al., 1998) observations indicate positively charged flowing potential structures. It is

important to note that a potential structure, whether positive or negative, must inherently be a part of some nonlinear wave where the charges are trapped, otherwise it would rapidly disrupt due to the repulsive forces of the charges. Depending on the free energy available, some of the instabilities discussed in the previous section could evolve nonlinearly into solitary waves, for example, whistler-type solitons. If this happens it would naturally explain the recent observations on the waveform of the coherent structures (including the associated magnetic component, if any) as reported by POLAR (Mozer et al., 1997; Franz et al., 1998) and FAST (Ergun et al., 1998) teams.

The high time resolution measurements of the broadband plasma waves in the PCBL region by POLAR and in the auroral ionosphere by FAST have just started to come out, and they have given very useful information on the fine structure of the BL waves. Further analyses of the high time resolution plasma and wave data from POLAR, FAST and Geotail would advance our knowledge about the generation and saturation mechanisms of the BL waves as well as about their fine structures. This would lead to better understanding about the BL waves and their role in cross-field particle diffusion leading to the formation of the boundary itself, and in the process of heating/acceleration and precipitation of the BL plasma causing the dayside aurora.

Acknowledgment

Portions of this research effort were performed at the Jet Propulsion Laboratory, California Institute of Technology, Pasadena, under contract with the National Aeronautics and Space Administration.

References

Akasofu, S.-I., Hones, Jr., E. W., Bame, S.J., Asbridge, J.R., and Lui, A.T.Y.: 1973, 'Magnetotail and boundary layer plasma at geocentric distance of 18R_E: Vela 5 and 6 observations', *J. Geophys. Res.* **78**, 7257.

Akimoto, K. and Omidi, N.: 1986, 'The generation of broadband electrostatic noise by an ion beam in the magnetotail', *Geophys. Res. Lett.* **13**, 97.

Anderson, B.J.: 1995, 'ULF signals observed near the magnetopause in Physics of the magnetopause', in P. Song, B.U.O. Sonnerup, and M.F. Thomsen, (eds.), *Physics of the Magnetopause*, *AGU Monograph* **90**, AGU, Washington, D.C., p. 269.

Anderson, K.A., Binsack, J.H., and Fairfield, D.H.: 1968, 'Hydromagnetic disturbances of 3 to 15 minute period on the magnetopause and their relation to Bow Shock Spikes', *J. Geophys. Res.* **73**, 2371.

Anderson, R.R., Harvey, C.C., Hoppe, M.M., Tsurutani, B.T.: 1968, Eastman, T.E., and Etcheto, J.: 1982, 'Plasma waves near the magnetopause', *J. Geophys. Res.* **87**, 2087.

Ashour-Abdalla, M. and Kennel, C.F.: 1978, 'Nonconvective and convective electron cyclotron harmonic instabilities', *J. Geophys. Res.* **83**, 1531.

Ashour-Abdalla, M. and Thorne, R.M.: 1977, 'The importance of electrostatic ion cyclotron instability for quiet-time proton auroral precipitation', *Geophys. Res. Lett.* **4**, 45.

Ashour-Abdalla, M. and Thorne, R.M.: 1978, 'Towards a unified view of diffuse auroral precipitation', *J. Geophys. Res.* **83**, 4775.

Aubry, M.P., Kivelson, M.G., and Russell, C.T., 'Motion and structure of the Magnetopause', *J. Geophys. Res.* **76**, 1673.

Axford, W.I. and Hines, C.O.: 1961, 'A unifying theory of high-latitude geophysical phenomena and geomagnetic storms', *Can. J. Phys.* **39**, 1433.

Axford, W.I.: 1964, 'Viscous interaction between the solar wind and the earth's magnetosphere', *Planet. Space Sci.* **13**, 45.

Bahnsen, A.: 1978, 'Recent techniques of observations and results from the magnetopause regions', *J. Atmospheric Terrest. Phys.* **40**, 235.

Baumjohann, W. and Paschmann, G.: 1987, 'Solar wind magnetosphere coupling, processes and observations', *Physica Scripta* **T18**, 61.

Belmont, G., Rebeau, F. and Rezeau, L.: 1995, 'Resonant amplification of magnetosheath MHD fluctuations at the magnetopause', *Geophys. Res. Lett.* **22**, 295.

Bohm, D.: 1949, 'Quantitative description of the arc plasma in the magnetic field, in A. Guthrie and R. Walkerling (eds.), *Characteristics of Electrical Discharges in Magnetic Fields*, p. 1, McGraw Hill, New York.

Catto, P.J., Rosenbluth, M.N., and Liu, C.S.: 1973, 'Parallel velocity shear instabilities in an inhomogeneous plasma with a sheared magnetic field', *Phys. Fluids* **16**, 1719.

Cattel, C.A., Mozer, F.S., Anderson, R.R., Hones, Jr., E.W., and Sharp, R.D.:1986, 'ISEE observations of the plasma sheet boundary, plasma sheet, and neutral sheet, 2, waves', *J. Geophys. Res.* **91**, 5681.

Cattell, C., Wygant, J., Mozer, F.S., Okada, T., Tsuruda, K., Kokubun, S., and Yamamoto, T.: 1995, 'ISEE 1 and Geotail observations of low-frequency waves at the magnetopause', *J. Geophys. Res.* **100**, 11823.

Chandrasekhar, S.:1961, *Hydrodynamic and Hydromagnetic Stability*, Clarendon, Oxford.

Chmyrev, V.M., Bilichenko, S.V., Pokhotelov, O.A., Marchenko, V.A., Lazarev, V.I. Streltsov, A.V., and Stenflo, L., Alfvén vortices and related phenomena in the ionosphere and the magnetosphere', *Phys. Scr.* **38**, 841.

Cummings, W.D. and Coleman, P.J., Jr.: 1968, 'Magnetic fields in the magnetopause and vicinity at synchronous altitude', *J. Geophys. Res.* **73**, 5699.

D'Angelo, N.: 1965, 'Kelvin–Helmholtz instability in a fully ionized plasma in a magnetic field', *Phys. Fluids* **8**, 1748.

D'Angelo, N.: 1973, 'Ultra low-frequency fluctuations at the polar cusp: A review', *Rev. Geophys.* **15**, 299.

Davidson, R.C.: 1978, 'Quasilinear stabilization of lower-hybrid drift instability', *Phys. Fluids* **21**, 1375.

Drake, J.F.: 1995, 'Magnetic reconnection, a kinetic treatment', in *Physics of the Magnetopause*, *Geophys. Mon.* **90**, Amer. Geophys. Union, Washington, DC, p. 155.

Drake, J.F., Gerber, J., and Kleva, R.G.: 1994a, 'Turbulence and transport in the magnetopause current layer', *J. Geophys. Res.* **99**, 11211.

Drake, J.F., Kleva, R.G., and Mandt, M.E.: 1994b, 'Structure of thin current layers: Implications for magnetic reconnection', *Phys. Rev. Lett.* **73**, 1251.

Dubouloz, N., Pottelette, R., Malingre, M., Holingren, G., and Lindqvist, P.A.: 1991, 'Detailed analysis of broadband electrostatic noise in the dayside auroral zone', *J. Geophys. Res.* **96**, 3565.

Dum, C.T.: 1989, 'Transition in the dispersive properties of beam-plasma and two-stream instabilities', *J. Geophys. Res.* **94**, 2429.

Dum, C.T., and Dupree, T.H.: 1970, 'Nonlinear stabilization of high-frequency instabilities', *Phys. Fluids* **13**, 2064.

Eastman, T.E., Hones, Jr., E.W., Bame, S.J., and Asbridge, J. R.: 1976, 'The magnetospheric boundary layer: Site of plasma, momentum and energy transfer, from the magnetosheath into magnetosphere', *Geophys. Res. Lett.* **3**, 685.

Ergun, R.: 1998, 'FAST satellite observations of large amplitude solitary structures', *Geophys. Res. Lett.* **25**, 2041.

Eviatar, A. and Wolf, R.A.: 1968, 'Transfer processes in the magnetopause', *J. Geophys. Res.* **73**, 5561.

Fairfield, D.H.: 1976, 'Magnetic fields of the magnetosheath', *Rev. Geophys. Space Phys.* **14**, 117.

Franz, J.R., Kintner, P.M., and Pickett, J.S.:1998, 'Polar observations of coherent electric field structures', *Geophys. Res. Lett.* **25**, 1277.

Ganguli, G., Keskinen, M.J., Romero, H., Heelis, R., Moore, T., and Pollock, C.: 1994, 'Coupling of microprocesses and macroprocesses due to velocity shear: An application to the low-altitude ionosphere', *J. Geophys. Res.* **99**, 8873.

Gary, S.P. and Eastman, T.E.: 1979, 'The lower hybrid drift instability at the magnetopause', *J. Geophys. Res.* **84**, 7378.

Gary, S.P. and Sgro, A.G.: 1990, 'The lower hybrid drift instability at the magnetopause', *J. Geophys. Res.* **17**, 909.

Gary, S.P., Smith, C.W., Lee, M.A., Goldstein, M.L., and Forslundd D.W.: 1984, 'Electromagnetic ion beam instabilities', *Phys. Fluids* **27**,1852. (Erratum, *Phys. Fluids* **28**, 438,1985).

Gendrin, R.: 1979, 'Magnetic turbulence and diffusion processes in the magnetopause boundary layer', *J. Geophys. Res.* **84**, 7043.

Gendrin, R.: 1983, 'Magnetic turbulence and diffusion processes in the magnetopause boundary layer', *Geophys. Res. Lett.* **10**, 769.

Gurnett, D.A., Frank, L.A., and Lepping, R.P.: 1976, 'Plasma waves in the distant magnetotail', *J. Geophys. Res.* **81**, 6059.

Gurnett, D.A. and Frank, L.A.: 1977, 'A region of intense plasma wave turbulence on auroral field lines', *J. Geophys. Res.* **82**, 1031.

Gurnett, D.A., and Frank, L.A.: 1978, 'Plasma waves in the polar cusp: Observations from Hawkeye 1', *J. Geophys. Res.* **82**, 1447.

Gurnett, D.A., Anderson, R.R., Tsurutani, B.T., Smith, E.J., Paschmann, G., Haerendel, G., Bame, S.J., and Russell, C.T.: 1979, 'Plasma wave instabilities at the magnetopause: Observations from ISEE 1 and 2', *J. Geophys. Res.* **84**, 7043.

Gurnett, D.A., Huff, R.L., Menietti, J.D., Burch, J.L., Winningham, J.D., and Shawhan, S.D.: 1984, 'Correlated low-frequency electric and magnetic noise along the auroral field lines', *J. Geophys. Res.* **89**, 897.

Gurnett, D.A. et al.: 1995, 'The Polar plasma wave instrument', *Space Sci. Rev.* **71**, 597.

Gonzalez, W.D., Tsurutani, B.T., Gonzalez, A.L.C., Smith, E.J., Tang, F., and Akasofu, S.-I.: 1989, 'Solar wind magnetosphere coupling during intense magnetic storms (1978–1979)', *J. Geophys. Res.* **94**, 8835.

Haerendel, G. and Paschmann, G.: 1982, 'Interaction of the solar wind with the dayside magnetosphere', in A. Nishida (ed.), *Magnetospheric Plasma Physics*, Center for Academic Publications Japan, Tokyo.

Haerendel, G., Paschmann, G., Sckopke, N, Rosenbauer, H., and Hedgecock, P. C.: 1978, 'The frontside boundary layer of the magnetopause and the problem of reconnection', *J. Geophys. Res.* **83**, 3195.

Ho, C.M., Tsurutani, B.T., Gurnett, D.A., Pickett, J.S.: 1997, 'Wideband plasma waves in the polar cap boundary layer: Polar observations, *Proceedings of Third SOLTIP Symposium*, Beijing, in press.

Holzer, R.E., Mcleod, M.G., and Smith, E.J.: 1966, 'Preliminary results from the Ogo 1 search coil magnetometer: Boundary positions and magnetic noise spectra', *J. Geophys. Res.* **71**, 1481.

Hones, E.W., Jr., Asbridge, J.R., Bame, S.J., Montgomery, M.D., Singer, S., and Akasofu, S.-I.: 1972, 'Measurements of the magnetotail plasma flow made by VELA-4B', *J. Geophys. Res.* **77**, 5503.

Huba, J.D.: 1981, 'The Kelvin–Helmholtz instability in inhomogeneous plasma', *J. Geophys. Res.* **86**, 3653.

Huba, J.D., Gladd, N.T., and Drake, J.F.: 1981, 'On the role of the lower hybrid drift instability in substorm dynamics', *J. Geophys. Res.* **86**, 5881.

Ichimaru, S.: 1973, *Basic Principles of Plasma Physics*, W. A. Benjamin, New York.

Johnson, J.R. and Cheng, C.Z.: 1997, Global structure of mirror modes in the magnetosheath', *J. Geophys. Res.* **102**, 7179.

Kennel, C.F. and Ashour-Abdalla, M.: 1982, 'Electrostatic Waves and the Strong Diffusion of Magnetospheric Electrons, in A. Nishida (ed.), *Magnetospheric Plasma Physics*, Center for Academic Publications Japan, Tokyo, p. 245.

Kennel, C.F., and Petschek, H.E.: 1966, 'Limit on stably trapped particle fluxes', *J. Geophys. Res.* **71**, 1.

Kindel, J.M. and Kennel, C.F.: 1971, 'Topside current instabilities', *J. Geophys. Res.* **76**, 3055.

Kojima, H., Matsumoto, H., Chikuba, S., Horiyama, S., Ashour-Abdalla, M., and Anderson, R.R.: 1997, 'Geotail waveform observations of broadband/narrowband electrostatic noise in the distant tail', *J. Geophys. Res.* **102**, 14439.

LaBelle, J., and Treumann, R.A.: 1988, 'Plasma waves at the dayside magnetopause', *Space Sci. Revs.* **47**, 175.

Lakhina, G.S.: 1987, 'Low-frequency electrostatic noise due to velocity shear instabilities in the regions of magnetospheric flow boundaries', *J Geophys. Res.* **92**, 12161.

Lakhina, G.S.: 1993, 'Generation of low-frequency electric field fluctuations on auroral field lines', *Annales Geophysicae* **64**, 660.

Lakhina, G.S.: 1994, 'Linear macroscopic instabilities in space plasmas', *Phys. Scripta* **T50**, 114.

Lakhina, G. S. and Sen, A.: 1973, 'Electromagnetic and ∇B effects on the modified two stream instability, *Nucl. Fusion* **13**, 913.

Lakhina, G.S. and Schindler, K.: 1996, 'Tearing modes at the magntopause', *J. Geophys. Res.* **101**, 2707.

Lakhina, G.S., Shukla, P.K., and Stenflo, L.: 1993, 'Ultra-low-frequency fluctuations at the magnetopause', *Geophys. Res. Lett.* **20**, 2419.

Lakhina, G.S., and Tsurutani, B.T.: 1999, 'A generation mechanism for the polar cap boundary layer broadband plasma waves', *J. Geophys. Res.* **104**, 279.

Lakhina, G.S. Tsurutani B.T., Arballo, J.K., Ho, C.M., and Boonsiriseth, A.: 1997, 'Generation of broadband plasma waves in the polar cap boundary layer', *EOS, Trans. AGU* **78**, S297.

Lundin, R.: 1987, 'Processes in the magnetospheric boundary layer', *Physica Scripta* **18**, 85,1987.

Matsumoto, H., Kojima, H., Miyatake, T., Omura, Y., Okada, M., and Tsutsui: 1994, 'Electrostatic solitary waves (ESW) in the magnetotail-BEN BEN wave forms observed by GEOTAIL', *Geophys. Res. Lett.* **21**, 2915.

McBride, J.B., E. Ott, E.,. Boris, J.P., and Orens, J.H.: 1972, 'Theory and simulation of turbulent heating by the modified two-stream instability', *Phys. Fluids* **15**, 2367.

Miura, A.: 1987, 'Simulation of the Kelvin–Helmholtz instability at the magnetospheric boundary', *J. Geophys. Res.* **92**, 3195.

Mozer, F.S., Ergun, R., Temerin, M., Cattell, C., Dombeck, J., and Wygant, J.: 1997, 'New features of time domain electric-field structures in the auroral acceleration region', *Phys. Rev. Lett.* **79**, 1281.

Neugebauer, M., Russell, C.T., and Smith, E.J.: 1974, 'Observations of the internal structure of the magnetopause', *J. Geophys. Res.* **79**, 499.

Omura, Y., Matsumoto, H., Miyake, T., and Kojima, H.: 1996, 'Electron beam instabilities as generation mechanism of electrostatic solitary waves in the magnetotail', *J. Geophys. Res.* **101**, 2685.

Papadopoulos, K.: 1979, 'The role of microturbulence on collisionless reconnection, in S.I. Akasofu (ed.), *Dynamics in the Magnetosphere*, D. Reidel Publishing. Co., Dordrecht, Holland, p. 289.

Pickett, J.S., Anderson, R.R., Frank, L.A. Gurnett, D.A., Paterson, W.R., Scudder, J.D., Sigworth, J.B., Tsurutani, B.T., Ho, C.M., Lakhina, G.S., Peterson, W.K., Shelley, E.G., Russell, C.T., Parks, G.K., Brittnacher, M.J., Matsumoto, H., Hashimoto, K., Nagano, I., Kokubun, S., and Yamamoto, T.: 1997, II. 'Correlative magnetopause boundary layer observations', *EOS* **78**, S291.

Pottelette, R., Malingre, M., Dubouloz, N., Aparicio, B., Lundin, R., Holmgren, G., and Marklund, G.: 1990, 'High-frequency waves in the cusp/cleft regions', *J. Geophys. Res.* **95**, 5957.

Revathy, P. and Lakhina, G.S.: 1977, 'Ion and electron heating in the Earth's bow shock', *J. Plasma Phys.* **17**, 133.

Rezeau, L., Morane, A., Perraut, S., Roux, A., and Schmidt, R.: 1989, 'Characterization of Alfvénic fluctuations in the magnetopause boundary layer', *J. Geophys. Res.* **94**, 101.

Rezeau, L., Perraut, S., and Roux, A.: 1986, 'Electromagnetic fluctuations in the vicinity of the magnetopause', *Geophys. Res. Lett.* **13**, 1093.

Rome, J.A. and Briggs, R., 1972, 'Stability of sheared electron flow' *Phys. Fluids* **15**, 796.

Rönnmark, K., Borg, H., Christiansen, P.J., Gough, M.P., and Jones, D.: 1978, 'Banded electron cyclotron harmonic instability – A first comparison of theory and experiment', *Space Sci. Rev.* **22**, 401.

Rosenbauer, H., Grunwaldt, H., Montgomery, M.D., Paschmann, G., and Sckopke. N.: 1975, 'HEOS 2 plasma observations in the distant polar magnetosphere: The Plasma Mantle', *J. Geophys. Res.* **80**, 2723.

Russell, C.T., Snare, R.C., Means, J.D., Pierce, D. Dearborn, D., Larson, M., Barr, G., and Le, G.: 1995, 'The GGS/POLAR magnetic fields investigation', *Space Sci. Revs.* **71**, 563.

Scarf, F.L., Fredricks, R.W., Green, I.M., and Russell, C.T.: 1972, 'Plasma waves in the dayside polar cusp', *J. Geophys. Res.* **77**, 2274.

Sckopke, N.G., Paschmann, G., Harendel, G., Sonnerup, B.U.O., Bame, S.J., Forbes, T.G., Hones, Jr., E.W., and Russell, C.T.: 1981, 'Structure of the low-latitude boundary layer', *J. Geophys. Res.* **86**, 2099.

Shelley, E.G. et al.: 1995,'The toroidal imaging mass-angle spectrograph (TIMAS) for the Polar Mission', *Space Sci. Rev.* **71**, 497.

Smith, E.J. and Davis, L.: 1970, 'Magnetic measurements in the Earth's magnetopause and magnetosheath: Mariner 5', *J. Geophys. Res.* **75**, 1233.

Song, P., Zhu, J., Russell, C.T., Anderson, R.R., Gurnett, D.A., Ogilvie, K.W., and Strangeway, R.J.: 1998, 'Properties of ELF emission in the dayside magnetopause', *J. Geophys. Res.* **103**, 26495.

Sonnerup, B.U.O.: 1980, 'Theory of the low latitude boundary layer', *J. Geophys. Res.* **85**, 2017.

Swift, D.F.: 1977, 'Turbulent generation of electrostatic fields in the magnetosphere', *J. Geophys. Res.* **82**, 5143.

Thorne, R.M. and Tsurutani, B.T.: 1991, 'Wave-particle interactions in the magnetopause boundary layer, in T. Chang et al. (ed.), *Physics of Space Plasmas (1990)*, Sci. Publ. Inc., Cambridge, MA, **10**, 119.

Treumann, R.A.: 1997, 'Theory of super-diffusion for the magnetopause', *Geophys. Res. Lett.* **24**, 1727.

Treumann, R.A., LaBelle, J., and Bauer, T.M.: 1995, 'Diffusion processes: An observational perspective', in *Physics of the Magnetopause*, Geophys. Mon. 90, Amer. Geophys. Union, Washington, DC, 331.

Treumann, R.A., LaBelle, J., and Pottelette, R.: 1991, 'Plasma diffusion at the magnetopause, The case of lower hybrid drift waves', *J. Geophys. Res.* **96**, 16009.

Tsurutani, B.T., Brinca, A.L., Smith, E.J., Okida, R.T., Anderson, R.R., and Eastman, T.E.: 1989, 'A statistical study of ELF-VLF plasma waves at the magnetopause', *J. Geophys. Res.* **94**, 1270.

Tsurutani, B.T. and Gonzalez, W.D.: 1995, 'The efficiency of "viscous interaction" between the solar wind and the magnetosphere during intense northward IMF events', *Geophys. Res. Lett.* **22**, 663.

Tsurutani, B.T. and Lakhina, G.S.: 1997, 'Some basic Concepts of wave-particle interaction in collisionless plasmas', *Rev. Geophys.* **35**, 491.

Tsurutani, B.T., Lakhina, G.S., Ho, C.M., Arballo, J.K., Galvan, C., Boonsiriseth, A., Pickett, J.S., Gurnett, D.A., Peterson, W.K., and Thorne, R.M.: 1998, 'Broadband plasma waves observed in the polar cap boundary layer (PCBL): Polar', *J. Geophys. Res.* **103**, 17351.

Tsurutani, B.T., Smith, E.J., Thorne, R.M., Anderson, R.R., Gurnett, D.A., Parks, G.K., Lin, C.S., and Russell, C.T.: 1981, 'Wave-particle interaction at the magnetopause: Contribution to the dayside aurora', *Geophys. Res. Lett.* **8**, 183.

Tsurutani, B.T., and Thorne, R.M.: 1982, 'Diffusion processes in the magnetopause boundary layer', *Geophys. Res. Lett.* **22**, 663.

Verheest, F. and Lakhina, G.S.: 1991, 'Nonresonant low-frequency instabilities in multibeam plasmas: Applications to cometary environments and plasma sheet boundary layers', *J. Geophys. Res.* **96**, 7905.

Verheest, F. and Lakhina, G.S.: 1993, 'Resonant electromagnetic ion-ion beam turbulence at comet P/Grigg-Skjellerup', *J. Geophys. Res.* **98**, 21,017.

Weiss, L.A., Reiff, P.H., Moses, J.J., and Moore, B.D.: 1992, 'Energy dissipation in substorms', Eur. Space Agency Spec. Publ., ESA-SP-335, 309.

Winske, D. and Omidi, N.: 1995, 'Diffusion at the magnetopause: hybrid simulations', *J. Geophys. Res.* **100**, 11,923.

Winske, D., Thomas, V.A., and Omidi, N.: 1995, 'Diffusion at the magnetopause: A theoretical perspective, in Physics of the Magnetopause, Geophys. Mon. 90, Amer. Geophys. Union, Washington, DC, 321.

Young, T.S.T., Callen, J.D., and McCune, J.E.: 1973, 'High frequency electrostatic waves in the magnetosphere', *J. Geophys. Res.* **78**, 1082.

Zhu, Z., Song, P., Drake, J.F., Russell, C.T., Anderson, R.R., Gurnett, D.A., Ogilvie, K.W., and Fitzenreiter, R.J.: 1996, 'The relationship between ELF-VLF waves and magnetic shear at the dayside magnetopause', *Geophys. Res. Lett.* **23**, 773.